R. & M. No. 2741
(12,647)
A.R.C. Technical Report

MINISTRY OF SUPPLY

AERONAUTICAL RESEARCH COUNCIL
REPORTS AND MEMORANDA

Low-Speed Measurements of the Pressure Distribution at the Surface of a Swept-back Wing

By
V. M. FALKNER, B.Sc., A.M.I.Mech.E.,
and
DORIS E. LEHRIAN, B.Sc.,
of the Aerodynamics Division, N.P.L.

LONDON: HER MAJESTY'S STATIONERY OFFICE
1953
FOUR SHILLINGS NET

Low-Speed Measurements of the Pressure Distribution at the Surface of a Swept-back Wing

By

V. M. Falkner, B.Sc., A.M.I.Mech.E.,

and

Doris E. Lehrian, B.Sc.,

of the Aerodynamics Division, N.P.L.

*Reports and Memoranda No. 2741**

November, 1949

Summary.—Low-speed measurements of the pressure distribution have been made at selected stations on a swept-back wing with and without body. The wing was of 45 deg sweep-back, with a sharp discontinuity at the centre-section, and of aspect ratio 3 with uniform chord. The aerofoil section was chosen to be suitable for work at low Reynolds number, and the wing plan to be of the maximum utility for comparison of observed and calculated pressure distribution. The work is the first part of a programme designed to give results of the greatest assistance to the development of mathematical methods, and the model was of exceptionally clean design to avoid extraneous effects.

The symmetry of the model allowed the work to be duplicated by covering a range of positive and negative incidences, and by averaging, it has been possible to remove zero irregularities due to wind-tunnel flow and present accurate values of pressure distribution, distribution of local lift coefficient and centre of pressure of normal force for a range of incidence 0 to 16 degrees. Wind-tunnel balance measurements of overall lift appear to be in reasonable agreement with the pressure plots.

A selection of chordwise pressure distributions is plotted and it is shown that at zero lift for the wing along there is good agreement with curves calculated at the Royal Aircraft Establishment. A comparison of a potential solution for load grading and local aerodynamic chord with the wind-tunnel measurements at finite lift shows approximately the variation due to the effects of wing thickness and viscosity.

1. *Introduction.*—The work described in this report forms the first part of a programme being carried out on a swept-back wing in order to provide a check on methods of calculating the pressure at the surface, as well as the general properties of wings. Much useful information has been provided by the application of methods of calculation based on potential theory, but it is essential to have accurate measurements of pressure distribution on a wing to guide developments of the theory which seek, with a minimum of complication, to allow for effects such as discontinuity in plan, the addition of a body to the wing, and the effects of wing thickness and viscosity.

The programme of pressure plotting is a lengthy one, but the report covers a definite and useful field which includes what is thought to be one of the worst types of discontinuity likely to require investigation, (excluding separate developments such as deflected flaps) ; that is, sudden change in direction of both leading and trailing edges of the wing. The work has been carried out on a 45 deg swept-back wing of uniform chord with nearly square tips, and includes pressure plotting and balance measurements of lift and moment with and without a body. Provision has been made for another position of the body relative to the wing, and for alternative rounded wing tips, and further work relating to these variations will follow.

1.1. Theoretical calculations of pressure distribution with finite lift have not yet been carried to a stage where they can be presented comprehensively, and so only the values required to show two comparisons of general interest have been included. (Figs. 11 and 12.) The first shows the near agreement of the measured pressure distribution at zero lift with some calculations

* Published with the permission of the Director, National Physical Laboratory.

made at the Royal Aircraft Establishment. The other is a comparison of the measured distribution of local lift coefficient and aerodynamic centre, at small values of C_L, with the theoretical values obtained by an eight-point solution on a thin wing of the same plan form. This comparison serves to show the order of difference in these quantities due to the effects of wing thickness and viscosity, and any appreciable wind-tunnel interference and residual wing tip effect.

The wing and the general pattern of the tests and analysis have been designed primarily for detailed comparison with theoretical calculations of load distribution, and should not be judged from any other aspect.

2. *Description of Wing*.—The wing is flat and symmetrical, of uniform chord, aspect ratio 3, and with 45 deg of sweepback as shown in Fig. 1, the shape being the result of careful choice with the object of obtaining results of the widest possible general use. Among the points considered were the necessity for the sharp discontinuity at the median section in both leading and trailing edges in order to assist an important and decisive numerical development (*see* R. & M. 2596[1]); the advantage of the 45 deg of sweep and uniform chord in providing as nearly as possible the rectangular framework likely to be most suitable in the treatment of the problem by networks, either numerically as, for example, in relaxation, or experimentally, as with a grid of electric currents; and the necessity for an aspect ratio low enough to conform to modern practice, but not so low as to cause the effects of the discontinuity to lose their distinctive properties (*see* R. & M. 2596[1]) and so spoil one of the objects of the work. Another advantage of the low aspect ratio is that it allows for the use of a reasonable chord on a wing with area small enough to be used in a 7 ft wind tunnel, without introducing into the magnitude of the wind-tunnel interference corrections uncertainties which could only be resolved by inconveniently long calculations.

The work has been carried out at a low Reynolds number, of order $0 \cdot 4 \times 10^6$ and, although, as far as possible, an aerofoil section suitable for this purpose has been used, the uniform chord is of further advantage in helping to eliminate errors due to variable local Reynolds number in the wind tunnel. In order to minimise the excess lift and irregularities due to flow over the wing tips, to which attention was first drawn by Sir Melvill Jones in R. & M. 73 (1913)[2], and which have since been shown to be worst with square tips, the ends were rounded off so that all vertical sections parallel to the leading edge end with a semi-circle struck on the thickness as diameter.

The results of the tests confirm that any residual effects due to this cause are small, but, because of the importance of the elimination of this phenomenon, which would otherwise introduce mathematical complications, provision has been made for further tests on alternative wing tips. The chord for these tips is rounded off elliptically to zero from a position 0·5 chord inboard of the tip, and they should remove any residual effects, perhaps at the expense of slight error due to variable local Reynolds number.

Although the rounding of the square tips reduces slightly the wing area, the analysis has all been based on the area of 3 sq ft.

2.1. It was necessary to use an aerofoil section suitable for work at low Reynolds number, and that chosen, in the wind direction, was a Piercy symmetrical aerofoil, 12·08 per cent thick, with the maximum thickness fairly far forward at 0·271 chord. This section has also been used by Dr. A. S. Halliday for whirling-arm models and the writers are indebted to Mr. A. R. Curtis for communicating the analysis and calculations relating to this section. In terms of the original report on these aerofoils by Piercy, Piper and Preston[3], (1937) the values of the parameters are as follows:—
$\varepsilon \doteq -\frac{1}{2}$, $\sigma\pi = 0 \cdot 08929$. Half-angle of trailing edge $= 5 \cdot 115$ deg. $dC_L/d\alpha$ in potential flow $= 1 \cdot 0974 \times 2\pi$. Position of aerodynamic centre $= 0 \cdot 2578$ chord. Maximum $t/c = 12 \cdot 08$ per cent at $0 \cdot 271$ chord.

The ordinates of the aerofoil of 12 in. chord are given in Table 1, and a diagram in Fig. 2.

3. *Description of Body*.—A body of revolution is used with the profile derived from a Young high-speed section. The chord is 40 in., fineness ratio 0·15, and maximum diameter at 0·35 chord, and the proportionate size to the wing was chosen as being representative of modern practice.

The profile of the body to full size, and a plan of the symmetrical wing and body combination, as tested, are given in Table 3 and Fig. 3 respectively. The body is here placed in the forward position with the nose 11·0 in. forward of the wing apex, but, as no theory would be permanently acceptable unless based on at least two body positions, provision has been made for later tests with the body in the rear position with the nose 5 in. forward of the wing apex.

4. *Pressure Plotting Arrangements*.—In order to limit the work to reasonable proportions, it was decided to pressure plot at six stations only parallel to the wind direction. To overcome the well-known difficulty in pressure plotting of the occasional unexplained bad reading, the work was duplicated by placing pressure holes on both surfaces of the half-wing and covering a complete range of positive and negative angles.

For the wing as shown in Fig. 1, the first two Stations A and B were duplicates positioned as near as possible to the line of symmetry, each being displaced $\frac{1}{4}$ in. from this line. The remainder of the sections C, D, E and F were placed at 0·25, 0·5, 0·75 and 0·875 of the semi-span. The pressure holes were located at even fractions of the chord, and Table 2 gives the positions of the holes both as fractions of the chord and as offset distances from the chord.

For the wing and body as shown in Fig. 3, the Station A is located along the centre-line of the body, and Station B on the line of intersection with the body of a plane $0 \cdot 125s$ or 2·25 in. distant from the median plane. The location of the pressure holes as a fraction of the chord and as a vertical offset from the chord line for these two stations is given in Table 4. Stations C to F are in the same position as for the wing alone.

4.1. In order to ensure accuracy, it was specified that the outlet pressure tubes should interfere as little as possible with the flow and should be clear of the critical region of the discontinuity. The work of designing the general arrangement of the pressure tubes and the suspension was undertaken by Mr. T. H. Fewster of Aerodynamics Division. The writers are indebted to Mr. Fewster for the considerable amount of time and skill given to this problem, as a result of which a design was evolved which must surely be one of the cleanest and most successful yet produced. It was necessary to limit the number of manometer leads to two per spanwise station, making 12 in all, and these were placed in conduits in sets of six before passing to the two streamline tubes containing the copper tubing which conveyed the pressure to a multitube manometer below the wind tunnel. The streamline tubes, which are of a section $0 \cdot 75 \times 0 \cdot 30$ in., pass through the wing surface and the connections inside the wing are made with valve rubber. They are shown in Fig. 4, which gives a sketch of the arrangement of the wing in the wind tunnel. Careful arrangements were also made for the change-over of pressure tubes with a minimum of trouble when the body was coupled to the wing in either forward or rear position. A photograph of the wing and body is shown in Fig. 5.

5. *Balance Measurements*.—The tests were made in the 7 ft No. 2 Wind Tunnel at 65 ft/sec, giving a Reynolds number of $0 \cdot 41 \times 10^6$, and a ratio of wing area to tunnel area of 6·1 per cent.

Measurements of lift, drag and moment for the wing, the wing and body combination, and the body alone, were made on the balance. The arrangement of the wing in the wind tunnel for these balance tests was as shown in Fig. 4 for the pressure plotting, excepting that the two streamline tubes under the model were omitted in order to avoid constraint on the model. This work is being carried out in alternation with other work on swept-back wings, but particular care has been taken to ensure that the wind tunnel is always in the same condition before further tests are made. That this arrangement has been successful is shown by the measurements on the wing given in Table 5, which repeated almost exactly after an interval of 5 months. The agreement also shows that the model must be free from any change in shape due to distortion.

The measurements for the wing and body are given in Table 6, and for the body alone in Table 7, and all three sets of readings, which refer to the uncorrected measurements in the wind tunnel, are plotted in Fig. 6. The moment axis for the wing alone, and the wing and body, was 10·5 in. behind the apex of the wing, but for the body alone was at the quarter-chord, or 10 in. behind the nose.

The analysis for the tests of Tables 5 and 6 is based on a wing area of 3 sq ft, and a mean chord of 12 in. For the body alone, the coefficients are based on the vertical projected area of 1·141 sq ft and the projected mean chord of 2·281 ft.

The results show that the tests are free from such irregularities as laminar separation, which would invalidate comparison with theory.

6. *Pressure Plotting*.—The measured pressure coefficients for the wing, in terms of the velocity head at the position of the model in the empty wind tunnel, are given in Tables 8 to 13. The normal force, the moment, and the centre of pressure of normal force at each station, were obtained by numerical integration. The tangential-force coefficient was obtained by plotting the observations against Y and integrating numerically, and the lift and drag coefficients by resolving the forces in the usual way. In carrying out this resolution, the zero for incidence was taken to be the local zero for the station determined by zero normal force. The results for the six stations are given in Tables 14 to 16.

A similar set of observations and deduced coefficients for the wing and body is given in Tables 17 to 25. For Stations A and B the primary observations refer to chords of 40 and 20·8 in. respectively, but for convenience the coefficients of lift and drag are also expressed with reference to the 12 in. chord.

6.1. Although figures for drag have been given in these tables, it must be stressed that these are incidental to the work and are to be used as a guide rather than as accurate values. The first main object of the work is to consider lift distribution and it is well known that even if it were worth serious consideration at low Reynolds number, the accurate measurement of local drag is a long and difficult matter, particularly when the influence of viscosity is included. In plotting the pressure coefficients against Y it was frequently necessary to estimate the run of the curves, and, although this was done in a consistent manner many more pressure holes would be required if a specified accuracy in the tangential force coefficient were required.

6.2. The first part of the theoretical work now in progress, but not included in this report, is concerned mainly with conditions when C_L is small. The measured values of the centre of pressure have therefore been plotted over the full range for the two tests in Figs. 7 and 8, but, due to lack of perfect symmetry at $C_L = 0$, the calculated values in this region will tend to move to infinity. It is possible to estimate the values for symmetry at $C_L = 0$ by drawing continuous curves through the points. This has been done for both sets and the values for zero incidence, or nearly enough for zero lift, indicated. It will be noted that the results are more spread for the wing and body tests and show the greatest variation at Station A along the body centre. It is unlikely that this variation is all due to lack of symmetry in the model or wind tunnel, and there is probably some reluctance on the part of the airflow to establish symmetry when the body is present.

6.3. The local lift coefficients for the two tests have been plotted in Figs. 9 and 10.

It will be seen from the results at zero incidence that there is a small directional wind error in the tunnel, coupled with a slight rotation of the air stream, or a slight permanent distortion of the model, alone or in combination. If the zero error is eliminated by using the results for incidence 0 as the datum, the points for positive and negative incidences plot very well, and the mean curves are then as drawn in the lower part of Figs. 9 and 10. It will be found that there is a slight difference in the angle for zero lift as given by the balance readings and the pressure plotting, and it has been confirmed by a special test that this can be accounted for partly by the omission of the streamline tubes under the wing during the balance tests. The zero variation for the balance readings is eliminated in the same way by using mean values of C_L for positive and negative incidence, and values obtained thus, representing the mean C_L over the wing, are given also in the lower diagrams of Figs. 9 and 10.

The curves of Fig. 10 have been completed by dotted lines in order to indicate that, if great accuracy were required over the body and wing root, it would be necessary to use more Stations. The general trend of the curves conforms to general knowledge of the subject, the drop in loading over the body being necessarily followed by a rise centred about the critical chord at 2·31 in. from the centre, or $\eta = 0 \cdot 128$, where the trailing edge of the wing joins the body.

6.4. In addition to the irregularities which have been eliminated by using the results for zero incidence as the datum, there are further irregularities in the detailed pressure plotting due to C_m and C_L not being zero simultaneously. These errors can be eliminated by applying a correction to the pressure coefficients based on the use of the mean pressure of upper and lower surfaces at zero incidence. That this procedure is accurate is shown by the fact that the answers are little different from the same means for ± 2 deg. For example, the pressure distribution at the median section and at half semi-span for the wing alone, and for the wing and body, at 0 and 8 deg incidence may be considered.

In Table 26 are given the mean pressure coefficients for upper and lower surface at Station A for $-$ 2, 0, and 2 deg, derived from Table 8, and the absence of any marked variation in the three results shows that the mean values for 0 deg can be used with confidence to represent the observations for true symmetrical flow. A similar averaging procedure applied to finite angles of incidence, reduces, using 8 deg as an example, to taking the mean of U for 8 deg and L for $-$ 8 deg as the true value of the upper coefficient, and the mean of L for 8 deg and U for $-$ 8 deg as the value of the lower coefficient. The final values for the wing alone for 0 deg and 8 deg at two stations are given under the headings ' Mean of A and B ' and ' Station D '.

Similar results for wing and body derived from Tables 17 and 20 are given in Table 27.

These figures have been plotted in Fig. 11, in which are also included calculations of the pressure distribution at Stations A and D for the wing alone at zero incidence which were made by Miss Weber at the Royal Aircraft Establishment, and communicated to the writer by Mr. R. Hills.

7. *Conclusions.*—As far as the integrated characteristics of the wing are concerned, the main conclusions are as represented in the lower diagrams of Figs. 9 and 10, where, with zero irregularities removed, the mean curves for positive and negative angles of incidence are believed to represent to close accuracy the distribution of local lift coefficient, based on the 12 in. chord, along the span. There is a little uncertainty in the curves for wing and body, but general knowledge favours the shapes indicated.

An approximate integration of the curves of Figs. 9 and 10 suggests that the agreement between average lift coefficients as given by balance and pressure plotting is reasonable. A proper examination of this agreement will involve not only theoretical treatment of wing loading, but a study of the effects of viscosity, and is beyond the scope of the report.

It is a matter of general interest to indicate how nearly the measured values of local lift coefficient and aerodynamic centre agree with values obtained by potential theory. The wind-tunnel observations of these quantities at small C_L are plotted in Fig. 12 against theoretical potential values for a thin wing obtained from an eight-point solution. There is a displacement of the local aerodynamic centre and a distortion of the C_{LL} curve, but there should be no difficulty in accounting for these variations.

Examples are given in Tables 26 and 27, and Fig. 11, of how zero errors may be removed simply from the tables of pressure coefficients. It is interesting to note that, even though the influence of viscosity has not been included in the theory, there is very fair agreement between the pressure distributions as given by theory and experiment for two stations of the wing at zero lift.

The writers are convinced that the results given here will be of material assistance to the theory of wing loading as well as to aircraft designers and they recommend continuation and extension of the programme.

8. *Acknowledgements*.—The writers wish to acknowledge that the success of the work is in no small part due to the skill displayed by Mr. F. Miles in constructing an accurate and rigid model and to Mr. E. A. Wheeler, who made and fitted the metal parts connected with the pressure tubes and leads.

Acknowledgements are also due to Misses S. D. Brown and W. M. Tafe for extensive help in wind-tunnel observations and the subsequent analysis.

REFERENCES

No.	*Author*	*Title, etc.*
1	V. M. Falkner and D. Lehrian ..	Calculated Loadings due to Incidence of a Number of Straight and Swept-back wings. R. & M. 2596. June, 1948.
2	B. M. Jones and C. J. Paterson ..	Investigation of the Distribution of Pressure over the Entire Surface of an Aerofoil. R. & M. 73. 1913.
3	N. A. V. Piercy, R. W. Piper and J. H. Preston.	A New Family of Wing Profiles. *Phil. Mag.*, vol. 24, p. 425, 1937.

TABLE 1

Profile of Piercy Symmetrical Aerofoil, 12·08 *per cent thick,* 12 *in. Chord*

X inches	*Y* inches	*X* inches	*Y* inches
0·000	0·000	5·017	0·669
0·123	0·212	5·408	0·641
0·244	0·294	6·072	0·595
0·477	0·400	6·848	0·527
0·917	0·527	7·445	0·470
1·324	0·602	8·053	0·409
1·702	0·651	9·040	0·304
2·054	0·682	9·632	0·240
2·834	0·719	10·308	0·168
3·500	0·723	11·210	0·075
4·075	0·711	11·696	0·028
4·576	0·692	12·000	0·000

TABLE 2

Location of Pressure Holes at the Surface of a Piercy Aerofoil. Stations A, B, C, D, E, F for Tests on Wing Only; C, D, E, F for Tests on Wing and Body

Hole number	Fraction of chord	*Y* inches	Hole number	Fraction of chord	*Y* inches
1	0·0125	0·233	9	0·25	0·722
2	0·025	0·325	10	0·3	0·721
3	0·0375	0·391	11	0·4	0·679
4	0·050	0·443	12	0·5	0·600
5	0·075	0·522	13	0·6	0·494
6	0·10	0·584	14	0·7	0·373
7	0·15	0·662	15	0·8	0·245
8	0·20	0·702	16	0·9	0·115

TABLE 3

Profile of Body of Revolution Based on Young High-Speed Section, 15 *per cent Fineness Ratio,* 40 *in. Chord*

X inches	*Y* radius inches	*X* inches	*Y* radius inches
0	0	22	2·628
1	1·088	24	2·440
2	1·511	26	2·220
4	2·060	28	1·976
6	2·428	30	1·704
8	2·692	32	1·404
10	2·864	34	1·076
12	2·964	36	0·724
14	3·000	38	0·360
16	2·976	39	0·184
18	2·900	40	0
20	2·780		

TABLE 4

Location of Pressure Holes at the Surface of a Body. Stations A and B in tests of Wing and Body

Hole number	Fraction of chord	A Central section 40″ chord Y inches	B Section 2·25″ from centre 20·8″ chord Y inches	Hole number	Fraction of chord	A Central section 40″ chord Y inches	B Section 2·25″ from centre 20·8″ chord Y inches
0	0	0	0	10	0·30	2·964	1·877
1	0·0125	0·773	0·477	11	0·40	2·976	1·969
2	0·0250	1·088	0·643	12	0·50	2·780	1·969
3	0·0375	1·323	0·776	13	0·60	2·440	1·869
4	0·050	1·511	0·891	14	0·70	1·976	1·700
5	0·075	1·817	1·067	15	0·80	1·404	1·428
6	0·10	2·060	1·221	16	0·90	0·724	1·055
7	0·15	2·428	1·456	17	0·95	0·360	0·760
8	0·20	2·692	1·633	18	1·00	0	0
9	0·25	2·864	1·766				

TABLE 5

45 deg V-wing, Aspect Ratio 3. Wind-Tunnel Balance Measurements

13 JULY, 1948			11 DECEMBER, 1948		
W. T. Inc. degrees	C_L	C_m	W. T. Inc. degrees	C_L	C_m
− 20·55	− 1·098	0·1115	− 9·15	− 0·447	0·0273
− 19·30	− 1·010	0·1350	− 6·80	− 0·336	0·0196
− 13·55	− 0·653	0·0443	− 4·45	− 0·224	0·0128
− 7·85	− 0·382	0·0221	− 2·20	− 0·109	0·0071
− 2·00	− 0·104	0·0058	0·10	0·004	0·0032
3·70	0·182	− 0·0042	2·40	0·116	− 0·0002
9·40	0·464	− 0·0216	4·70	0·228	− 0·0059
15·20	0·745	− 0·0505	6·50	0·321	− 0·0114
21·15	1·015	− 0·1058	7·90	0·389	− 0·0159
− 19·95	− 1·016	0·1258			
− 16·60		0·0751			
12·30		− 0·0307			
19·20	1·043	− 0·1482			
− 20·40	− 0·990	0·1153			
− 17·40		0·0972			
− 14·65	− 0·703	0·0517			
− 11·72		0·0356			
− 8·80	− 0·426	0·0264			
− 5·92		0·0161			
− 3·05	− 0·144	0·0084			
− 0·28		0·0031			
2·50	0·133	− 0·0016			
5·40		− 0·0090			
8·30	0·416	− 0·0191			
11·20		− 0·0271			
14·10	0·693	− 0·0401			
17·02		− 0·0781			
19·95	1·101	− 0·1623			

TABLE 6

45 deg V-wing, Aspect Ratio 3, with Body. Wind-Tunnel Balance Measurements

APRIL 1949			APRIL 1949		
W. T. Inc. Degrees	C_L	C_m	W. T. Inc. Degrees	C_L	C_m
− 16	− 0·854	0·0584	− 16	− 0·854	0·0587
− 12	− 0·632	0·0254	− 10	− 0·528	0·0196
− 8	− 0·424	0·0153	0	− 0·004	0·0050
− 4	− 0·209	0·0075	10	0·515	− 0·0082
			16	0·843	− 0·0404
0	− 0·005	0·0047	− 20	− 1·046	0·1060
2	0·099	0·0042	− 18	− 0·990	0·0999
4	0·208	0·0019	17·7	0·993	− 0·0864
8	0·418	− 0·0052	19·7	1·094	− 0·1145
12	0·614	− 0·0115			
16	0·842	− 0·0414	− 20	− 1·046	0·1060
			− 18	− 0·990	0·0999
− 16	− 0·852	0·0583	17·7	0·993	− 0·0864
− 12	− 0·633	0·0251	19·7	1·094	− 0·1145
− 8	− 0·417	0·0151			
− 4	− 0·211	0·0071			
− 2	− 0·107	0·0053			
0	− 0·004	0·0045			
2	0·099	0·0040			
4	0·205	0·0022			
8	0·421	− 0·0054			
12	0·619	− 0·0113			
16	0·852	− 0·0401			

TABLE 7

Body Only. Wind-Tunnel Balance Measurements

W. T. Inc. Degrees	C_L	C_m	C_D	W. T. Inc. Degrees	C_L	C_m	C_D
− 20·5	− 0·071	− 0·028	0·0433	2·1	0·005	0·006	0·0195
− 18·5	− 0·060	− 0·029	0·0388	3·9	0·016	0·010	0·0200
− 16·5	− 0·050	− 0·029	0·0344	5·7	0·024	0·014	0·0218
− 14·5	− 0·042	− 0·028	0·0294	7·6	0·027	0·019	0·0240
− 12·6	− 0·036	− 0·026	0·0261	9·6	0·028	0·022	0·0251
− 10·7	− 0·028	− 0·024	0·0229	11·6	0·035	0·025	0·0257
− 8·8	− 0·016	− 0·021	0·0204	13·5	0·042	0·027	0·0280
− 7·0	− 0·012	− 0·017	0·0195	15·4	0·054	0·028	0·0312
− 5·2	− 0·009	− 0·013	0·0188	17·4	0·063	0·029	0·0375
− 3·3	− 0·003	− 0·008	0·0184	19·4	0·070	0·029	0·0419
− 1·4	0·002	− 0·004	0·0193	21·3	0·078	0·029	0·0473
0·3	0·005	0·002	0·0197				

TABLE 8

Wing Only. Observed Pressure Coefficients at Station A

Tunnel Inci-dence	−16		−12		−8		−4		−2		0		2		4		8		12		16	
Point	L	U	L	U	L	U	L	U	L	U	L	U	L	U	L	U	L	U	L	U	L	U
1	−1·099	0·768	−0·693	0·735	−0·328	0·663	−0·015	0·521	0·123	0·422	0·256	0·307	0·364	0·193	0·473	0·048	0·602	−0·265	0·732	−0·633	0·783	−1·054
2	−1·145	0·783	−0·780	0·702	−0·461	0·572	−0·157	0·407	−0·021	0·301	0·120	0·181	0·241	0·060	0·334	−0·069	0·533	−0·355	0·678	−0·678	0·783	−1·045
3	−1·145	0·753	−0·822	0·627	−0·506	0·482	−0·214	0·289	−0·096	0·181	0·051	0·048	0·166	−0·069	0·271	−0·187	0·425	−0·461	0·630	−0·753	0·750	−1·084
4	−1·169	0·693	−0·852	0·557	−0·572	0·386	−0·301	0·196	−0·169	0·090	−0·042	−0·030	0·072	−0·142	0·181	−0·262	0·373	−0·512	0·545	−0·798	0·696	−1·114
5	−1·166	0·617	−0·864	0·467	−0·608	0·295	−0·361	0·105	−0·241	0·000	−0·127	−0·114	−0·024	−0·220	0·081	−0·325	0·331	−0·557	0·443	−0·810	0·602	−1·114
6	−1·024	0·557	−0·828	0·407	−0·572	0·241	−0·361	0·066	−0·253	−0·039	−0·145	−0·142	−0·048	−0·235	0·039	−0·337	0·226	−0·560	0·392	−0·804	0·548	−0·964
7	−0·913	0·467	−0·747	0·316	−0·584	0·163	−0·392	0·000	−0·301	−0·090	−0·205	−0·187	−0·111	−0·271	−0·030	−0·361	0·139	−0·542	0·304	−0·705	0·461	−0·873
8	−0·889	0·407	−0·711	0·259	−0·572	0·111	−0·407	−0·045	−0·325	−0·127	−0·235	−0·211	−0·157	−0·292	−0·072	−0·361	0·084	−0·524	0·241	−0·660	0·392	−0·828
9	−0·813	0·355	−0·684	0·211	−0·542	0·069	−0·404	−0·075	−0·325	−0·151	−0·241	−0·232	−0·175	−0·310	−0·102	−0·383	0·048	−0·506	0·196	−0·639	0·340	−0·771
10	−0·768	0·319	−0·642	0·187	−0·512	0·048	−0·392	−0·090	−0·319	−0·166	−0·244	−0·241	−0·181	−0·301	−0·105	−0·376	0·033	−0·491	0·181	−0·602	0·316	−0·723
11	−0·660	0·259	−0·545	0·136	−0·446	0·012	−0·346	−0·105	−0·295	−0·181	−0·238	−0·238	−0·181	−0·301	−0·111	−0·352	0·012	−0·443	0·142	−0·548	0·265	−0·648
12	−0·587	0·223	−0·506	0·111	−0·404	0·000	−0·325	−0·102	−0·277	−0·157	−0·220	−0·211	−0·175	−0·256	−0·120	−0·301	−0·012	−0·383	0·099	−0·458	0·211	−0·548
13	−0·485	0·196	−0·419	0·096	−0·334	0·003	−0·250	−0·087	−0·238	−0·127	−0·184	−0·175	−0·145	−0·217	−0·090	−0·247	−0·003	−0·316	0·093	−0·377	0·205	−0·446
14	−0·386	0·190	−0·328	0·105	−0·271	0·015	−0·199	−0·057	−0·172	−0·090	−0·148	−0·127	−0·114	−0·154	−0·078	−0·181	0·003	−0·235	0·096	−0·292	0·181	−0·331
15	−0·268	0·181	−0·226	0·105	−0·181	0·033	−0·136	−0·027	−0·111	−0·048	−0·090	−0·078	−0·072	−0·090	−0·039	−0·114	0·030	−0·166	0·093	−0·196	0·175	−0·232
16	−0·130	0·160	−0·111	0·096	−0·087	0·054	−0·060	0·015	−0·054	−0·006	−0·036	−0·015	−0·024	−0·030	−0·006	−0·045	0·045	−0·075	0·096	−0·096	0·154	−0·108

L = Lower Surface. U = Upper surface.

TABLE 9

Wing Only. Observed Pressure Coefficients at Station B

Tunnel Incidence	−16		−12		−8		−4		−2		0		2		4		8		12		16	
Point	L	U	L	U	L	U	L	U	L	U	L	U	L	U	L	U	L	U	L	U	L	U
1	−1·024	0·765	−0·611	0·735	−0·259	0·669	0·045	0·530	0·181	0·434	0·302	0·325	0·401	0·211	0·509	0·075	0·642	−0·235	0·747	−0·593	0·765	−1·024
2	−1·066	0·777	−0·729	0·702	−0·373	0·572	−0·090	0·407	0·045	0·295	0·181	0·175	0·280	0·054	0·377	−0·078	0·557	−0·373	0·693	−0·708	0·789	−1·090
3	−1·142	0·747	−0·810	0·620	−0·503	0·479	−0·211	0·292	−0·078	0·181	0·057	0·054	0·178	−0·060	0·283	−0·181	0·476	−0·461	0·639	−0·765	0·753	−1·114
4	−1·157	0·693	−0·834	0·560	−0·554	0·395	−0·289	0·205	−0·154	0·096	−0·030	−0·024	0·075	−0·136	0·187	−0·256	0·377	−0·512	0·545	−0·807	0·696	−1·130
5	−1·120	0·617	−0·840	0·470	−0·572	0·301	−0·337	0·105	−0·217	0·003	−0·108	−0·114	−0·006	−0·220	0·099	−0·325	0·283	−0·557	0·452	−0·813	0·605	−1·130
6	−0·970	0·557	−0·819	0·401	−0·572	0·235	−0·364	0·054	−0·256	−0·048	−0·151	−0·160	−0·057	−0·253	0·033	−0·355	0·220	−0·578	0·386	−0·825	0·548	−1·003
7	−0·916	0·467	−0·759	0·319	−0·596	0·163	−0·398	0·000	−0·307	−0·090	−0·214	−0·184	−0·117	−0·271	−0·036	−0·361	0·136	−0·554	0·301	−0·705	0·458	−0·867
8	−0·858	0·407	−0·705	0·259	−0·560	0·111	−0·398	−0·045	−0·313	−0·127	−0·226	−0·211	−0·151	−0·292	−0·066	−0·361	0·090	−0·524	0·244	−0·657	0·395	−0·825
9	−0·807	0·349	−0·673	0·205	−0·536	0·060	−0·392	−0·081	−0·319	−0·163	−0·235	−0·241	−0·172	−0·319	−0·096	−0·392	0·060	−0·524	0·199	−0·648	0·349	−0·789
10	−0·768	0·319	−0·642	0·187	−0·512	0·048	−0·392	−0·084	−0·319	−0·163	−0·244	−0·241	−0·181	−0·301	−0·105	−0·373	0·033	−0·491	0·181	−0·602	0·316	−0·723
11	−0·663	0·259	−0·551	0·136	−0·452	0·015	−0·349	−0·105	−0·295	−0·178	−0·238	−0·238	−0·181	−0·298	−0·117	−0·352	0·003	−0·443	0·136	−0·548	0·256	−0·648
12	−0·587	0·223	−0·512	0·111	−0·401	0·000	−0·325	−0·102	−0·277	−0·157	−0·223	−0·211	−0·175	−0·256	−0·120	−0·301	−0·009	−0·383	0·099	−0·464	0·220	−0·551
13	−0·485	0·193	−0·407	0·096	−0·328	0·003	−0·247	−0·087	−0·223	−0·127	−0·172	−0·175	−0·142	−0·220	−0·090	−0·250	−0·003	−0·322	0·093	−0·383	0·202	−0·452
14	−0·386	0·187	−0·328	0·105	−0·271	0·015	−0·199	−0·057	−0·172	−0·090	−0·148	−0·127	−0·114	−0·154	−0·078	−0·181	0·006	−0·235	0·096	−0·295	0·181	−0·337
15	−0·268	0·181	−0·226	0·105	−0·181	0·033	0·127	−0·027	−0·108	−0·048	−0·087	−0·078	−0·072	−0·090	−0·039	−0·114	0·030	−0·169	0·093	−0·199	0·175	−0·238
16	−0·133	0·169	−0·114	0·105	−0·090	0·060	−0·063	0·045	−0·054	−0·018	−0·039	0·009	−0·024	−0·006	−0·006	−0·018	0·045	−0·051	0·096	−0·069	0·151	−0·081

L = Lower surface. U = Upper surface.

TABLE 10

Wing Only. Observed Pressure Coefficients at Station C

Tunnel Incidence	−16		−12		−8		−4		−2		0		2		4		8		12		16	
Point	L	U	L	U	L	U	L	U	L	U	L	U	L	U	L	U	L	U	L	U	L	U
1	−2·922	0·069	−1·928	0·377	−1·069	0·494	−0·407	0·422	−0·148	0·307	0·087	0·130	0·271	−0·075	0·398	−0·331	0·518	−0·979	0·467	−1·777	0·241	−2·771
2	−2·783	0·392	−1·898	0·512	−1·190	0·473	−0·584	0·301	−0·316	0·163	−0·075	−0·030	0·111	−0·232	0·262	−0·482	0·461	−1·054	0·542	−1·732	0·500	−2·530
3	−2·723	0·518	−1·762	0·521	−1·169	0·410	−0·645	0·196	−0·398	0·039	−0·181	−0·166	−0·003	−0·355	0·148	−0·578	0·392	−1·099	0·524	−1·672	0·572	−2·440
4	−2·636	0·551	−1·672	0·497	−1·151	0·343	−0·693	0·105	−0·464	−0·051	−0·259	−0·241	−0·090	−0·428	0·066	−0·648	0·313	−1·090	0·482	−1·605	0·557	−2·380
5	−1·852	0·536	−1·633	0·422	−1·069	0·247	−0·678	0·015	−0·482	−0·127	−0·319	−0·292	−0·199	−0·458	−0·030	−0·623	0·217	−1·015	0·392	−1·536	0·518	−1·988
6	−1·605	0·491	−1·551	0·361	−1·009	0·187	−0·642	−0·030	−0·482	−0·163	−0·325	−0·301	−0·193	−0·437	−0·069	−0·578	0·163	−0·946	0·349	−1·325	0·482	−1·521
7	−1·310	0·422	−1·030	0·283	−0·873	0·114	−0·584	−0·075	−0·467	−0·181	−0·343	−0·301	−0·229	−0·407	−0·117	−0·527	0·072	−0·789	0·241	−0·961	0·392	−1·220
8	−1·093	0·367	−0·895	0·226	−0·699	0·072	−0·533	−0·093	−0·419	−0·187	−0·325	−0·286	−0·232	−0·377	−0·139	−0·473	0·030	−0·633	0·184	−0·807	0·331	−0·994
9	−0·952	0·313	−0·798	0·181	−0·623	0·039	−0·491	−0·105	−0·398	−0·196	−0·310	−0·271	−0·232	−0·355	−0·157	−0·443	0·000	−0·560	0·139	−0·702	0·280	−0·843
10	−0·834	0·277	−0·705	0·151	−0·563	0·015	−0·452	−0·114	−0·377	−0·181	−0·292	−0·265	−0·226	−0·331	−0·157	−0·413	−0·021	−0·509	0·117	−0·623	0·247	−0·753
11	−0·633	0·220	−0·542	0·108	−0·437	0·000	−0·337	−0·105	−0·301	−0·166	−0·247	−0·217	−0·193	−0·271	−0·127	−0·319	−0·021	−0·401	0·090	−0·482	0·211	−0·563
12	−0·488	0·187	−0·416	0·090	−0·346	0·000	−0·271	−0·090	−0·250	−0·133	−0·211	−0·190	−0·157	−0·217	−0·120	−0·241	−0·021	−0·316	0·066	−0·367	0·169	−0·443
13	−0·386	0·151	−0·301	0·069	−0·241	0·000	−0·187	−0·075	−0·151	−0·114	−0·142	−0·151	−0·127	−0·157	−0·090	−0·181	−0·012	−0·235	0·057	−0·271	0·151	−0·340
14	−0·283	0·139	−0·196	0·069	−0·151	0·021	−0·114	−0·045	−0·090	−0·072	−0·072	−0·060	−0·075	−0·084	−0·060	−0·108	0·000	−0·139	0·060	−0·172	0·127	−0·235
15	−0·193	0·127	−0·111	0·081	−0·069	0·039	−0·045	0·006	−0·036	0·015	−0·030	−0·012	−0·006	−0·030	0·000	−0·045	0·030	−0·060	0·066	−0·084	0·105	−0·157
16	−0·096	0·099	−0·048	0·063	−0·000	0·048	0·015	0·045	0·018	0·033	0·030	0·030	0·030	0·015	0·042	0·015	0·045	0·000	0·066	−0·030	0·093	−0·090

L = Lower surface. U = Upper surface.

TABLE 11

Wing Only. Observed Pressure Coefficients at Station D

Tunnel Incidence	−16		−12		−8		−4		−2		0		2		4		8		12		16	
Point	L	U	L	U	L	U	L	U	L	U	L	U	L	U	L	U	L	U	L	U	L	U
1	−3·178	−0·069	−2·154	0·316	−1·259	0·482	−0·512	0·437	−0·211	0·322	0·039	0·142	0·241	−0·075	0·386	−0·355	0·497	−1·069	0·422	−1·946	0·130	−3·042
2	−3·133	0·316	−1·952	0·491	−1·244	0·488	−0·657	0·337	−0·377	0·196	−0·127	0·000	0·060	−0·211	0·217	−0·470	0·446	−1·093	0·506	−1·843	0·452	−2·816
3	−2·795	0·470	−1·898	0·512	−1·265	0·431	−0·717	0·223	−0·476	0·069	−0·229	−0·136	−0·030	−0·346	0·123	−0·575	0·367	−1·120	0·506	−1·732	0·518	−2·696
4	−2·500	0·527	−1·843	0·497	−1·217	0·361	−0·744	0·130	−0·515	−0·030	−0·301	−0·223	−0·120	−0·422	0·036	−0·651	0·292	−1·120	0·452	−1·663	0·527	−2·590
5	−1·837	0·524	−1·657	0·428	−1·151	0·256	−0·729	0·036	−0·530	−0·114	−0·346	−0·286	−0·220	−0·446	−0·048	−0·627	0·196	−1·030	0·364	−1·514	0·482	−1·910
6	−1·575	0·485	−1·265	0·364	−1·102	0·199	−0·696	−0·021	−0·536	−0·145	−0·367	−0·292	−0·229	−0·428	−0·099	−0·578	0·133	−0·994	0·316	−1·265	0·440	−1·581
7	−1·250	0·407	−1·030	0·265	−0·864	0·108	−0·633	−0·075	−0·506	−0·187	−0·407	−0·307	−0·265	−0·416	−0·160	−0·542	0·036	−0·741	0·196	−0·988	0·337	−1·220
8	−1·009	0·325	−0·858	0·181	−0·708	0·033	−0·578	−0·130	−0·458	−0·226	−0·355	−0·325	−0·271	−0·413	−0·181	−0·512	−0·012	−0·693	0·136	−0·873	0·271	−1·030
9	−0·843	0·271	−0·726	0·139	−0·611	0·006	−0·518	−0·136	−0·413	−0·220	−0·331	−0·301	−0·256	−0·377	−0·187	−0·467	−0·039	−0·584	0·090	−0·723	0·220	−0·825
10	−0·717	0·232	−0·627	0·111	−0·530	−0·012	−0·449	−0·133	−0·386	−0·199	−0·304	−0·277	−0·241	−0·346	−0·172	−0·413	−0·051	−0·521	0·072	−0·617	0·187	−0·699
11	−0·509	0·187	−0·440	0·084	−0·389	−0·015	−0·307	−0·108	−0·307	−0·163	−0·247	−0·211	−0·196	−0·259	−0·142	−0·286	−0·054	−0·361	0·033	−0·422	0·142	−0·452
12	−0·404	0·151	−0·307	0·060	−0·262	−0·009	−0·217	−0·084	−0·175	−0·120	−0·187	−0·160	−0·148	−0·181	−0·114	−0·205	−0·030	−0·259	0·036	−0·283	0·111	−0·322
13	−0·361	0·120	−0·208	0·057	−0·181	−0·003	−0·148	−0·060	−0·117	−0·075	−0·093	−0·090	−0·090	−0·114	−0·090	−0·136	−0·027	−0·169	0·033	−0·181	0·090	−0·256
14	−0·289	0·105	−0·142	0·054	−0·102	0·012	−0·078	−0·024	−0·060	−0·036	−0·054	−0·045	−0·042	−0·060	−0·042	−0·078	−0·006	−0·090	0·030	−0·108	0·075	−0·220
15	−0·187	0·090	−0·087	0·063	−0·048	0·030	−0·030	0·015	−0·021	0·000	−0·009	−0·012	−0·003	−0·024	0·009	−0·030	0·018	−0·036	0·036	−0·060	0·054	−0·202
16	−0·078	0·069	−0·033	0·060	0·015	0·042	0·030	0·039	0·030	0·033	0·036	0·033	0·036	0·024	0·042	0·027	0·045	0·012	0·039	−0·030	0·036	−0·181

L = Lower surface. U = Upper surface.

TABLE 12

Wing Only. Observed Pressure Coefficients at Station E

Tunnel Incidence	−16		−12		−8		−4		−2		0		2		4		8		12		16	
Point	L	U	L	U	L	U	L	U	L	U	L	U	L	U	L	U	L	U	L	U	L	U
1	−3·313	−0·160	−2·199	0·271	−1·295	0·473	−0·548	0·461	−0·241	0·361	0·015	0·193	0·220	−0·030	0·367	−0·313	0·497	−1·042	0·422	−1·946	0·151	−3·042
2	−3·319	0·331	−2·072	0·470	−1·331	0·482	−0·720	0·331	−0·398	0·187	−0·145	−0·012	0·057	−0·229	0·235	−0·482	0·449	−1·099	0·506	−1·852	0·449	−2·741
3	−3·012	0·437	−1·973	0·497	−1·301	0·437	−0·753	0·250	−0·482	0·096	−0·238	−0·105	−0·045	−0·313	0·123	−0·542	0·361	−1·114	0·500	−1·762	0·512	−2·605
4	−2·304	0·497	−1·904	0·467	−1·265	0·346	−0·792	0·127	−0·548	−0·036	−0·337	−0·226	−0·151	−0·422	0·009	−0·642	0·265	−1·130	0·428	−1·672	0·506	−2·485
5	−1·883	0·497	−1·633	0·401	−1·145	0·247	−0·741	0·018	−0·548	−0·120	−0·377	−0·289	−0·214	−0·452	−0·075	−0·633	0·169	−1·018	0·337	−1·551	0·452	−2·078
6	−1·542	0·458	−1·235	0·337	−1·130	0·187	−0·693	−0·036	−0·524	−0·151	−0·361	−0·295	−0·235	−0·434	−0·105	−0·587	0·108	−0·952	0·280	−1·524	0·416	−1·416
7	−1·160	0·370	−1·006	0·241	−0·813	0·084	−0·611	−0·090	−0·482	−0·193	−0·367	−0·301	−0·259	−0·413	−0·163	−0·527	0·015	−0·729	0·181	−0·904	0·310	−1·114
8	−0·892	0·286	−0·819	0·163	−0·663	0·030	−0·542	−0·120	−0·437	−0·205	−0·346	−0·298	−0·265	−0·377	−0·181	−0·467	−0·030	−0·614	0·105	−0·771	0·226	−0·873
9	−0·678	0·223	−0·678	0·108	−0·572	−0·009	−0·482	−0·136	−0·392	−0·205	−0·313	−0·280	−0·256	−0·346	−0·187	−0·434	−0·060	−0·521	0·060	−0·633	0·172	−0·678
10	−0·536	0·175	−0·557	0·075	−0·488	−0·030	−0·410	−0·136	−0·361	−0·196	−0·289	−0·259	−0·235	−0·316	−0·181	−0·383	−0·078	−0·452	0·030	−0·527	0·120	−0·518
11	−0·361	0·108	−0·361	0·024	−0·328	−0·045	−0·265	−0·120	−0·256	−0·166	−0·235	−0·205	−0·190	−0·250	−0·142	−0·253	−0·066	−0·316	0·000	−0·346	0·075	−0·307
12	−0·307	0·066	−0·235	0·000	−0·220	−0·045	−0·184	−0·096	−0·163	−0·127	−0·151	−0·166	−0·145	−0·160	−0·117	−0·181	−0·063	−0·220	−0·021	−0·217	0·030	−0·220
13	−0·271	0·039	−0·139	−0·003	−0·127	−0·039	−0·120	−0·075	−0·117	−0·096	−0·087	−0·084	−0·087	−0·090	−0·090	−0·114	−0·060	−0·130	−0·003	−0·120	0·003	−0·181
14	−0·301	0·027	−0·075	0·000	−0·060	−0·018	−0·054	−0·045	−0·045	−0·039	−0·042	−0·036	−0·030	−0·048	−0·036	−0·051	−0·030	−0·060	−0·015	−0·060	0·000	−0·166
15	−0·319	0·015	−0·042	0·006	0·000	0·003	0·000	0·003	0·000	0·015	0·000	0·006	0·006	0·000	0·009	0·000	−0·012	−0·006	0·000	−0·021	−0·015	−0·172
16	−0·298	−0·018	−0·030	0·015	0·036	0·030	0·042	0·045	0·036	0·045	0·039	0·042	0·036	0·045	0·039	0·048	0·030	0·036	0·000	−0·003	−0·045	−0·199

L = Lower surface. U = Upper surface.

TABLE 13

Wing Only. Observed Pressure Coefficients at Station F

Tunnel Incidence	−16		−12		−8		−4		−2		0		2		4		8		12		16	
Point	L	U	L	U	L	U	L	U	L	U	L	U	L	U	L	U	L	U	L	U	L	U
1	−3·027	0·157	−1·988	0·401	−1·160	0·482	−0·476	0·377	−0·196	0·256	0·036	0·078	0·220	−0·136	0·364	−0·392	0·467	−1·036	0·392	−1·783	0·151	−2·636
2	−2·916	0·377	−1·901	0·470	−1·232	0·437	−0·608	0·271	−0·352	0·133	−0·105	−0·051	0·081	−0·256	0·232	−0·488	0·446	−1·048	0·482	−1·711	0·401	−2·455
3	−2·660	0·458	−1·813	0·467	−1·202	0·370	−0·663	0·172	−0·419	0·030	−0·184	−0·166	−0·012	−0·352	0·145	−0·563	0·361	−1·069	0·476	−1·611	0·482	−2·380
4	−2·485	0·467	−1·747	0·422	−1·205	0·301	−0·744	0·090	−0·512	−0·054	−0·316	−0·235	−0·145	−0·410	0·009	−0·608	0·250	−1·048	0·398	−1·527	0·467	−2·364
5	−1·747	0·437	−1·521	0·340	−1·169	0·187	−0·693	−0·018	−0·518	−0·151	−0·355	−0·301	−0·211	−0·449	−0·084	−0·614	0·142	−0·955	0·295	−1·458	0·404	−1·611
6	−1·367	0·370	−1·265	0·259	−1·015	0·120	−0·654	−0·072	−0·500	−0·175	−0·355	−0·301	−0·241	−0·422	−0·127	−0·557	0·066	−0·889	0·223	−1·175	0·343	−1·304
7	−0·988	0·250	−0·889	0·136	−0·729	0·012	−0·554	−0·136	−0·443	−0·217	−0·352	−0·307	−0·265	−0·398	−0·181	−0·491	−0·027	−0·684	0·105	−0·813	0·223	−0·946
8	−0·732	0·166	−0·702	0·066	−0·581	−0·036	−0·482	−0·151	−0·392	−0·217	−0·322	−0·286	−0·265	−0·349	−0·196	−0·422	−0·075	−0·533	0·030	−0·651	0·136	−0·711
9	−0·527	0·105	−0·560	0·018	−0·482	−0·072	−0·422	−0·160	−0·346	−0·211	−0·280	−0·262	−0·241	−0·313	−0·193	−0·383	−0·096	−0·440	−0·012	−0·527	0·075	−0·527
10	−0·398	0·060	−0·452	−0·009	−0·404	−0·084	−0·331	−0·157	−0·307	−0·196	−0·250	−0·241	−0·217	−0·280	−0·181	−0·316	−0·108	−0·380	−0·036	−0·434	0·030	−0·401
11	−0·247	0·012	−0·292	−0·048	−0·274	−0·078	−0·226	−0·120	−0·211	−0·151	−0·196	−0·175	−0·166	−0·196	−0·139	−0·193	−0·102	−0·241	−0·060	−0·271	−0·021	−0·223
12	−0·205	−0·012	−0·175	−0·051	−0·157	−0·069	−0·136	−0·093	−0·117	−0·111	−0·120	−0·114	−0·120	−0·114	−0·096	−0·127	−0·078	−0·160	−0·054	−0·163	−0·027	−0·151
13	−0·184	−0·030	−0·090	−0·054	−0·087	−0·060	−0·069	−0·066	−0·069	−0·060	−0·054	−0·060	−0·057	−0·060	−0·072	−0·075	−0·063	−0·084	−0·033	−0·090	−0·036	−0·136
14	−0·181	−0·030	−0·060	−0·036	−0·042	−0·036	−0·018	−0·018	−0·012	−0·015	−0·012	−0·006	−0·012	−0·006	−0·021	−0·009	−0·042	−0·024	−0·039	−0·045	−0·036	−0·145
15	−0·241	−0·042	−0·060	−0·030	0·003	−0·018	0·030	0·003	0·030	0·018	0·015	0·024	0·030	0·030	0·024	0·024	−0·018	0·006	−0·018	−0·036	−0·039	−0·196
16	−0·340	−0·078	−0·078	−0·021	0·015	0·009	0·051	0·039	0·054	0·054	0·054	0·060	0·048	0·066	0·048	0·066	0·030	0·030	−0·021	−0·045	−0·066	−0·256

L = Lower surface. U = Upper surface.

TABLE 14

Wing Only. Integrated Local Lift and Drag Coefficients, and Local Aerodynamic Centre

Station A. Chord 12 in.

Tunnel Incidence	Normal force	Tangential force	C_L	C_D	Local a.c.
− 16	− 0·860	− 0·0139	− 0·829	0·2280	0·347
− 12	− 0·649	0·0021	− 0·634	0·1404	0·344
− 8	− 0·438	0·0144	− 0·432	0·0776	0·340
− 4	− 0·229	0·0251	− 0·227	0·0422	0·337
− 2	− 0·125	0·0285	− 0·124	0·0335	0·350
0	− 0·012	0·0296	− 0·012	0·0297	—
2	0·089	0·0288	0·088	0·0314	0·303
4	0·196	0·0270	0·194	0·0396	0·326
8	0·405	0·0145	0·400	0·0687	0·338
12	0·611	0·0032	0·598	0·1271	0·340
16	0·820	− 0·0124	0·793	0·2100	0·343

Station B. Chord 12 in.

Tunnel Incidence	Normal force	Tangential force	C_L	C_D	Local a.c.
− 16	− 0·854	− 0·0123	− 0·823	0·228	0·350
− 12	− 0·646	0·0041	− 0·631	0·142	0·346
− 8	− 0·436	0·0179	− 0·429	0·081	0·343
− 4	− 0·229	0·0269	− 0·226	0·044	0·347
− 2	− 0·122	0·0293	− 0·121	0·034	0·364
0	− 0·010	0·0302	− 0·010	0·030	—
2	0·089	0·0297	0·088	0·032	0·283
4	0·195	0·0274	0·192	0·040	0·316
8	0·406	0·0165	0·400	0·071	0·334
12	0·611	0·0037	0·597	0·128	0·337
16	0·821	− 0·0132	0·794	0·210	0·341

TABLE 15

Wing Only. Integrated Local Lift and Drag Coefficients, and Local Aerodynamic Centre

Station C. Chord 12 in.

Tunnel incidence	Normal force	Tangential force	C_L	C_D	Local a.c.
− 16	− 0·924	− 0·1289	− 0·923	0·1373	0·283
− 12	− 0·696	− 0·0730	− 0·695	0·0780	0·268
− 8	− 0·466	− 0·0298	− 0·466	0·0387	0·259
− 4	− 0·247	− 0·0047	− 0·246	0·0142	0·254
− 2	− 0·133	0·0038	− 0·133	0·0094	0·257
0	− 0·018	0·0058	− 0·018	0·0059	—
2	0·087	0·0046	0·087	0·0070	0·240
4	0·200	− 0·0022	0·199	0·0103	0·249
8	0·415	− 0·0269	0·415	0·0283	0·254
12	0·624	− 0·0666	0·625	0·0603	0·260
16	0·858	− 0·1173	0·858	0·1176	0·275

Station D. Chord 12 in.

Tunnel incidence	Normal force	Tangential force	C_L	C_D	Local a.c.
− 16	− 0·849	− 0·1392	− 0·854	0·1092	0·269
− 12	− 0·628	− 0·0870	− 0·631	0·0520	0·243
− 8	− 0·438	− 0·0401	− 0·439	0·0258	0·229
− 4	− 0·244	− 0·0088	− 0·243	0·0108	0·224
− 2	− 0·136	− 0·0016	− 0·136	0·0046	0·219
0	− 0·027	0·0019	− 0·027	0·0022	—
2	0·076	0·0013	0·076	0·0032	0·237
4	0·177	− 0·0064	0·177	0·0041	0·222
8	0·376	− 0·0346	0·377	0·0141	0·225
12	0·568	− 0·0796	0·573	0·0343	0·228
16	0·792	− 0·1307	0·799	0·0844	0·258

TABLE 16

Wing Only. Integrated Local Lift and Drag Coefficients, and Local Aerodynamic Centre

Station E. Chord 12 in.

Tunnel incidence	Normal force	Tangential force	C_L	C_D	Local a.c.
− 16	− 0·763	− 0·1423	− 0·772	0·0815	0·265
− 12	− 0·541	− 0·0916	− 0·548	0·0286	0·197
− 8	− 0·380	− 0·0452	− 0·383	0·0121	0·182
− 4	− 0·214	− 0·0136	− 0·214	0·0036	0·180
− 2	− 0·123	− 0·0037	− 0·123	0·0019	0·189
0	− 0·027	0·0012	− 0·027	0·0015	—
2	0·062	0·0009	0·062	0·0024	0·178
4	0·151	− 0·0055	0·151	0·0035	0·179
8	0·319	− 0·0329	0·321	0·0085	0·179
12	0·487	− 0·0828	0·494	0·0152	0·181
16	0·658	− 0·1314	0·670	0·0482	0·217

Station F. Chord 12 in.

Tunnel incidence	Normal force	Tangential force	C_L	C_D	Local a.c.
− 16	− 0·594	− 0·1119	− 0·601	0·0613	0·228
− 12	− 0·436	− 0·0744	− 0·442	0·0218	0·169
− 8	− 0·304	− 0·0393	− 0·306	0·0060	0·148
− 4	− 0·161	− 0·0138	− 0·162	− 0·0011	0·134
− 2	− 0·089	− 0·0058	− 0·089	− 0·0019	0·143
0	− 0·016	− 0·0032	− 0·016	− 0·0031	—
2	0·051	− 0·0060	0·051	− 0·0047	0·099
4	0·121	− 0·0112	0·121	− 0·0038	0·125
8	0·256	− 0·0323	0·258	0·0014	0·139
12	0·393	− 0·0643	0·398	0·0154	0·161
16	0·525	− 0·1031	0·533	0·0409	0·208

(22974)

TABLE 17

Wing and Body. Observed Pressure Coefficients at Station A

Tunnel Incidence	−16		−12		−8		−4		−2		0		2		4		8		12		16	
Point	L	U	L	U	L	U	L	U	L	U	L	U	L	U	L	U	L	U	L	U	L	U
0	0·746	0·746	0·855	0·855	0·959	0·959	0·973	0·973	0·991	0·991	0·988	0·988	0·991	0·991	0·982	0·982	0·941	0·941	0·835	0·835	0·729	0·729
1	−0·313	0·777	−0·159	0·682	0·000	0·557	0·156	0·437	0·233	0·375	0·295	0·307	0·381	0·235	0·440	0·146	0·578	0·000	0·696	−0·137	0·802	−0·292
2	−0·357	0·595	−0·239	0·503	−0·124	0·378	0·003	0·244	0·083	0·199	0·142	0·125	0·204	0·057	0·268	0·006	0·401	−0·125	0·519	−0·235	0·622	−0·363
3	−0·351	0·476	−0·268	0·375	−0·162	0·256	−0·050	0·140	0·003	0·077	0·056	0·021	0·109	−0·027	0·165	−0·077	0·271	−0·185	0·389	−0·277	0·490	−0·378
4	−0·327	0·417	−0·248	0·312	−0·177	0·205	−0·080	0·110	−0·032	0·057	0·000	0·015	0·050	−0·033	0·112	−0·074	0·206	−0·170	0·316	−0·247	0·407	−0·315
5	−0·298	0·321	−0·242	0·235	−0·192	0·140	−0·115	0·042	−0·088	0·003	−0·041	−0·039	0·006	−0·065	0·032	−0·119	0·133	−0·182	0·230	−0·223	0·327	−0·283
6	−0·277	0·244	−0·245	0·170	−0·198	0·062	−0·139	−0·009	−0·115	−0·048	−0·077	−0·071	−0·035	−0·110	−0·009	−0·119	0·074	−0·196	0·165	−0·250	0·251	−0·283
7	−0·221	0·193	−0·186	0·116	−0·177	0·048	−0·133	−0·012	−0·100	−0·045	−0·091	−0·086	−0·056	−0·119	−0·012	−0·125	0·044	−0·182	0·109	−0·199	0·204	−0·226
8	−0·220	0·134	−0·202	0·068	−0·167	−0·003	−0·104	−0·060	−0·125	−0·092	−0·104	−0·122	−0·071	−0·137	−0·042	−0·158	0·015	−0·193	0·062	−0·217	0·140	−0·229
9	−0·217	0·131	−0·217	0·051	−0·185	−0·006	−0·155	−0·068	−0·131	−0·092	−0·122	−0·113	−0·098	−0·134	−0·068	−0·125	−0·015	−0·187	0·057	−0·199	0·134	−0·205
10	−0·241	0·131	−0·214	0·057	−0·190	−0·015	−0·155	−0·071	−0·125	−0·092	−0·098	−0·113	−0·092	−0·134	−0·060	−0·152	−0·009	−0·190	0·057	−0·199	0·128	−0·220
11	−0·345	0·161	−0·301	0·077	−0·257	0·003	−0·201	−0·068	−0·171	−0·098	−0·142	−0·131	−0·100	−0·164	−0·068	−0·190	−0·012	−0·226	0·074	−0·259	0·168	−0·312
12	−0·369	0·134	−0·330	0·051	−0·280	−0·015	−0·218	−0·083	−0·201	−0·119	−0·174	−0·137	−0·130	−0·161	−0·103	−0·193	−0·041	−0·229	0·041	−0·274	0·130	−0·310
13	−0·204	0·080	−0·180	0·021	−0·162	−0·021	−0·153	−0·065	−0·130	−0·080	−0·100	−0·083	−0·097	−0·104	−0·077	−0·122	−0·047	−0·140	0·015	−0·152	0·077	−0·176
14	−0·053	0·045	−0·059	0·009	−0·056	−0·009	−0·047	−0·018	−0·035	−0·027	−0·047	−0·039	−0·044	−0·042	−0·041	−0·036	−0·009	−0·024	0·015	−0·039	0·050	−0·042
15	0·053	0·021	0·041	0·015	0·021	0·012	0·015	0·018	0·015	0·018	0·018	0·021	0·012	0·033	0·012	0·027	0·018	0·039	0·021	0·051	0·018	0·057
16	0·100	0·065	0·097	0·062	0·074	0·060	0·083	0·060	0·071	0·071	0·074	0·068	0·071	0·074	0·065	0·077	0·065	0·086	0·047	0·113	0·071	0·116
17	0·097	0·092	0·094	0·095	0·097	0·089	0·071	0·086	0·071	0·095	0·083	0·092	0·068	0·098	0·074	0·089	0·080	0·104	0·083	0·104	0·086	0·107

L = Lower surface. U = Upper surface.

B*

TABLE 18

Wing and Body. Observed Pressure Coefficients at Station B

Tunnel Incidence	−16		−12		−8		−4		−2		0		2		4		8		12		16	
Point	L	U	L	U	L	U	L	U	L	U	L	U	L	U	L	U	L	U	L	U	L	U
0	−0·342	−0·342	−0·245	−0·245	−0·156	−0·156	−0·115	−0·115	−0·094	−0·094	−0·100	−0·100	−0·086	−0·086	−0·100	−0·100	−0·139	−0·139	−0·233	−0·233	−0·327	−0·327
1	−0·351	−0·250	−0·245	−0·164	−0·150	−0·116	−0·097	−0·077	−0·086	−0·068	−0·068	−0·068	−0·074	−0·083	−0·074	−0·101	−0·094	−0·158	−0·165	−0·229	−0·245	−0·345
2	−0·354	−0·244	−0·236	−0·140	−0·162	−0·095	−0·103	−0·068	−0·074	−0·060	−0·065	−0·071	−0·071	−0·080	−0·062	−0·098	−0·088	−0·149	−0·150	−0·229	−0·254	−0·342
3	−0·345	−0·205	−0·245	−0·137	−0·165	−0·077	−0·100	−0·060	−0·080	−0·068	−0·074	−0·068	−0·071	−0·080	−0·071	−0·107	−0·088	−0·161	−0·159	−0·241	−0·224	−0·351
4	−0·354	−0·202	−0·257	−0·128	−0·168	−0·080	−0·112	−0·060	−0·100	−0·062	−0·071	−0·068	−0·065	−0·089	−0·074	−0·107	−0·097	−0·167	−0·147	−0·247	−0·224	−0·345
5	−0·363	−0·196	−0·265	−0·128	−0·189	−0·092	−0·133	−0·071	−0·106	−0·080	−0·097	−0·083	−0·077	−0·098	−0·083	−0·125	−0·091	−0·187	−0·139	−0·259	−0·215	−0·360
6	−0·366	−0·232	−0·274	−0·131	−0·192	−0·098	−0·130	−0·083	−0·109	−0·083	−0·091	−0·104	−0·083	−0·113	−0·077	−0·101	−0·086	−0·185	−0·118	−0·262	−0·186	−0·363
7	−0·369	−0·208	−0·271	−0·158	−0·195	−0·119	−0·136	−0·104	−0·121	−0·107	−0·112	−0·128	−0·097	−0·137	−0·080	−0·158	−0·083	−0·214	−0·115	−0·295	−0·162	−0·375
8	−0·390	−0·161	−0·280	−0·119	−0·187	−0·089	−0·137	−0·095	−0·128	−0·098	−0·101	−0·116	−0·098	−0·128	−0·083	−0·149	−0·104	−0·208	−0·125	−0·286	−0·167	−0·381
9	−0·399	−0·149	−0·271	−0·101	−0·202	−0·089	−0·128	−0·077	−0·116	−0·089	−0·095	−0·104	−0·086	−0·119	−0·068	−0·113	−0·068	−0·199	−0·095	−0·274	−0·131	−0·390
10	−0·414	−0·116	−0·295	−0·086	−0·208	−0·068	−0·134	−0·065	−0·110	−0·071	−0·098	−0·098	−0·083	−0·113	−0·065	−0·131	−0·062	−0·199	−0·083	−0·283	−0·125	−0·396
11	−0·531	−0·009	−0·378	0·015	−0·248	0·006	−0·147	−0·018	−0·100	−0·039	−0·074	−0·065	−0·041	−0·104	−0·027	−0·152	0·009	−0·232	0·009	−0·354	−0·015	−0·515
12	−0·711	0·182	−0·552	0·131	−0·363	0·054	−0·239	−0·030	−0·180	−0·068	−0·139	−0·119	−0·083	−0·173	−0·032	−0·238	0·053	−0·348	0·130	−0·521	0·177	−0·765
13	−0·690	0·205	−0·546	0·131	−0·416	0·030	−0·304	−0·065	−0·248	−0·107	−0·183	−0·164	−0·133	−0·220	−0·088	−0·277	0·021	−0·369	0·115	−0·509	0·201	−0·631
14	−0·584	0·176	−0·501	0·077	−0·395	−0·015	−0·304	−0·110	−0·271	−0·158	−0·227	−0·211	−0·183	−0·241	−0·121	−0·280	−0·035	−0·357	0·062	−0·429	0·174	−0·515
15	−0·454	0·125	−0·398	0·051	−0·333	−0·033	−0·265	−0·116	−0·239	−0·149	−0·215	−0·152	−0·180	−0·214	−0·147	−0·244	−0·065	−0·307	0·024	−0·342	0·118	−0·402
16	−0·280	0·089	−0·263	0·024	−0·218	−0·024	−0·177	−0·071	−0·156	−0·095	−0·139	−0·110	−0·124	−0·128	−0·103	−0·161	−0·053	−0·190	0·024	−0·211	0·080	−0·241
17	−0·159	0·083	−0·153	0·024	−0·130	−0·012	−0·118	−0·045	−0·103	−0·045	−0·083	−0·065	−0·071	−0·074	−0·065	−0·083	−0·029	−0·122	0·024	−0·125	0·065	−0·137
18	0·006	0·006	0·015	0·015	0·018	0·018	0·024	0·024	0·024	0·024	0·024	0·024	0·024	0·024	0·024	0·024	0·024	0·024	0·024	0·024	0·021	0·021

L = Lower surface. U = Upper surface.

TABLE 19

Wing and Body. Observed Pressure Coefficients at Station C

Tunnel Incidence	−16		−12		−8		−4		−2		0		2		4		8		12		16	
Point	L	U	L	U	L	U	L	U	L	U	L	U	L	U	L	U	L	U	L	U	L	U
1	−3·218	−0·033	−2·156	0·339	−1·192	0·497	−0·445	0·411	−0·156	0·304	0·086	0·134	0·265	−0·110	0·410	−0·396	0·510	−1·119	0·410	−2·048	0·118	−3·112
2	−3·071	0·357	−1·979	0·512	−1·209	0·494	−0·566	0·295	−0·301	0·149	−0·083	−0·033	0·118	−0·271	0·274	−0·536	0·472	−1·170	0·534	−1·967	0·419	−2·994
3	−2·864	0·512	−1·885	0·551	−1·209	0·435	−0·658	0·193	−0·389	0·027	−0·183	−0·164	0·009	−0·387	0·168	−0·637	0·410	−1·199	0·525	−1·884	0·531	−2·845
4	−2·419	0·568	−1·832	0·500	−1·224	0·348	−0·711	0·095	−0·469	−0·074	−0·268	−0·262	−0·077	−0·476	0·071	−0·711	0·348	−1·223	0·499	−1·830	0·566	−2·560
5	−2·074	0·539	−1·693	0·440	−1·153	0·238	−0·711	−0·006	−0·540	−0·158	−0·351	−0·310	−0·180	−0·494	−0·029	−0·687	0·204	−1·110	0·407	−1·723	0·528	−1·997
6	−1·726	0·503	−1·404	0·372	−1·091	0·187	−0·658	−0·060	−0·496	−0·187	−0·342	−0·327	−0·198	−0·482	−0·065	−0·646	0·174	−1·045	0·345	−1·339	0·504	−1·655
7	−1·354	0·417	−1·121	0·271	−0·867	0·083	−0·611	−0·119	−0·481	−0·229	−0·357	−0·339	−0·245	−0·461	−0·124	−0·592	0·083	−0·833	0·245	−1·060	0·407	−1·321
8	−1·167	0·354	−0·961	0·202	−0·750	0·048	−0·565	−0·140	−0·443	−0·241	−0·354	−0·330	−0·241	−0·432	−0·155	−0·545	0·033	−0·714	0·199	−0·893	0·354	−1·077
9	−1·021	0·301	−0·863	0·158	−0·685	0·018	−0·542	−0·158	−0·437	−0·244	−0·357	−0·318	−0·259	−0·408	−0·170	−0·509	−0·024	−0·640	0·152	−0·801	0·289	−0·967
10	−0·920	0·262	−0·777	0·089	−0·628	−0·024	−0·491	−0·176	−0·417	−0·247	−0·333	−0·307	−0·259	−0·393	−0·179	−0·461	−0·036	−0·577	0·104	−0·711	0·259	−0·845
11	−0·737	0·196	−0·655	0·080	−0·534	−0·039	−0·422	−0·167	−0·381	−0·217	−0·310	−0·268	−0·248	−0·333	−0·189	−0·375	−0·065	−0·467	0·056	−0·574	0·183	−0·679
12	−0·634	0·164	−0·528	0·051	−0·437	−0·060	−0·339	−0·149	−0·336	−0·196	−0·277	−0·250	−0·224	−0·292	−0·201	−0·312	−0·074	−0·390	0·024	−0·470	0·136	−0·577
13	−0·513	0·128	−0·398	0·036	−0·333	−0·048	−0·271	−0·134	−0·254	−0·164	−0·236	−0·208	−0·183	−0·223	−0·133	−0·250	−0·071	−0·312	0·018	−0·369	0·118	−0·497
14	−0·386	0·116	−0·289	0·036	−0·239	−0·033	−0·183	−0·095	−0·156	−0·125	−0·139	−0·134	−0·150	−0·137	−0·097	−0·170	−0·041	−0·214	0·024	−0·253	0·109	−0·366
15	−0·271	0·104	−0·162	0·042	−0·142	0·000	−0·097	−0·036	−0·086	−0·036	−0·071	−0·036	−0·056	−0·068	−0·044	−0·080	−0·009	−0·125	0·029	−0·149	0·088	−0·247
16	−0·142	0·094	−0·091	0·053	−0·050	0·024	−0·009	0·021	−0·006	0·018	−0·012	−0·006	0·009	0·000	0·003	−0·012	0·024	−0·035	0·053	−0·059	0·083	−0·118

L = Lower surface. U = Upper surface.

TABLE 20

Wing and Body. Observed Pressure Coefficients at Station D

Tunnel Incidence	−16		−12		−8		−4		−2		0		2		4		8		12		16	
Point	L	U	L	U	L	U	L	U	L	U	L	U	L	U	L	U	L	U	L	U	L	U
1	−3·510	−0·185	−2·345	0·259	−1·336	0·449	−0·537	0·402	−0·233	0·301	0·027	0·113	0·221	−0·131	0·381	−0·452	0·463	−1·217	0·330	−2·214	−0·029	−3·399
2	−3·201	0·268	−2·088	0·429	−1·327	0·476	−0·649	0·312	−0·389	0·158	−0·136	−0·027	0·083	−0·265	0·239	−0·551	0·457	−1·220	0·487	−2·060	0·351	−3·190
3	−2·664	0·443	−2·021	0·506	−1·327	0·437	−0·696	0·199	−0·448	0·039	−0·212	−0·149	−0·032	−0·393	0·150	−0·643	0·375	−1·238	0·475	−1·967	0·442	−2·881
4	−2·431	0·503	−1·894	0·482	−1·307	0·351	−0·755	0·101	−0·513	−0·062	−0·310	−0·262	−0·118	−0·494	0·053	−0·738	0·322	−1·277	0·472	−1·905	0·504	−2·589
5	−1·965	0·506	−1·617	0·414	−1·183	0·238	−0·732	0·003	−0·531	−0·149	−0·354	−0·304	−0·186	−0·506	−0·027	−0·693	0·209	−1·152	0·413	−1·786	0·487	−2·018
6	−1·714	0·470	−1·398	0·360	−1·121	0·185	−0·720	−0·036	−0·549	−0·173	−0·398	−0·324	−0·239	−0·482	−0·100	−0·652	0·115	−1·104	0·316	−1·417	0·460	−1·664
7	−1·330	0·402	1·100	0·259	−0·897	0·095	−0·655	−0·116	−0·531	−0·226	−0·404	−0·339	−0·295	−0·458	−0·180	−0·589	0·029	−0·827	0·201	−1·054	0·348	−1·310
8	−1·104	0·312	−0·943	0·173	−0·744	0·018	−0·595	−0·164	−0·485	−0·256	−0·390	−0·345	−0·271	−0·452	−0·199	−0·562	−0·021	−0·735	0·128	−0·929	0·283	−1·080
9	−0·929	0·256	−0·804	0·134	−0·664	−0·015	−0·515	−0·176	−0·455	−0·253	−0·378	−0·327	−0·295	−0·414	−0·208	−0·503	−0·062	−0·637	0·092	−0·792	0·241	−0·887
10	−0·785	0·220	−0·694	0·104	−0·579	−0·042	−0·457	−0·167	−0·415	−0·241	−0·328	−0·310	−0·261	−0·384	−0·178	−0·461	−0·056	−0·571	0·075	−0·673	0·178	−0·738
11	−0·582	0·167	−0·516	0·068	−0·447	−0·033	−0·358	−0·140	−0·327	−0·185	−0·273	−0·235	−0·225	−0·310	−0·169	−0·312	−0·072	−0·399	0·023	−0·452	0·134	−0·518
12	−0·478	0·134	−0·363	0·048	−0·310	−0·036	−0·263	−0·107	−0·227	−0·152	−0·215	−0·196	−0·162	−0·211	−0·136	−0·232	−0·074	−0·295	−0·006	−0·315	0·103	−0·393
13	−0·404	0·101	−0·251	0·039	−0·218	−0·012	−0·168	−0·060	−0·139		−0·139		−0·106		−0·086		−0·044		0·012	−0·199	0·080	−0·336
14	−0·336	0·098	−0·165	0·045	−0·136	0·009	−0·091	−0·045	−0·077	−0·042	−0·065	−0·039	−0·047	−0·039	−0·044	−0·045	−0·009	−0·107	0·021	−0·122	0·077	−0·292
15	−0·242	0·077	−0·097	0·045	−0·056	0·030	−0·044	0·006	−0·027	0·012	−0·032	0·012	−0·018	0·015	−0·015	0·012	0·018	−0·048	0·021	−0·080	0·047	−0·262
16	−0·133	0·077	−0·038	0·053	0·009	0·035	0·015	0·041	0·038	0·027	0·021	0·032	0·041	0·041	0·018	0·041	0·024	0	0·018	−0·065	0·029	−0·221

L = Lower surface. U = Upper surface.

TABLE 21

Wing and Body. Observed Pressure Coefficients at Station E

Tunnel Incidence	−16		−12		−8		−4		−2		0		2		4		8		12		16	
Point	L	U	L	U	L	U	L	U	L	U	L	U	L	U	L	U	L	U	L	U	L	U
1	−3·608	−0·250	−2·345	0·214	−1·348	0·443	−0·560	0·405	−0·230	0·333	0·009	0·155	0·218	−0·074	0·369	−0·381	0·457	−1·146	0·327	−2·143	0·006	−3·268
2	−3·265	0·292	−2·183	0·461	−1·395	0·476	−0·693	0·312	−0·401	0·167	−0·162	−0·006	0·068	−0·232	0·248	−0·497	0·454	−1·161	0·490	−1·958	0·360	−3·051
3	−2·985	0·432	−2·097	0·497	−1·366	0·432	−0·755	0·226	−0·472	0·068	−0·251	−0·104	−0·044	−0·339	0·130	−0·595	0·369	−1·196	0·469	−1·937	0·460	−2·920
4	−2·510	0·485	−1·991	0·473	−1·357	0·327	−0·814	0·104	−0·569	−0·071	−0·366	−0·247	−0·150	−0·458	−0·003	−0·705	0·277	−1·238	0·451	−1·812	0·487	−2·601
5	−1·956	0·485	−1·575	0·405	−1·201	0·247	−0·755	−0·006	−0·501	−0·131	−0·378	−0·304	−0·218	−0·467	−0·056	−0·673	0·171	−1·092	0·369	−1·708	0·457	−1·917
6	−1·602	0·443	−1·289	0·342	−0·985	0·161	−0·693	−0·045	−0·516	−0·173	−0·366	−0·315	−0·221	−0·461	−0·088	−0·640	0·112	−1·051	0·289	−1·521	0·419	−1·583
7	−1·165	0·369	−1·009	0·244	−0·814	0·077	−0·614	−0·110	−0·481	−0·220	−0·354	−0·318	−0·251	−0·435	−0·150	−0·565	0·041	−0·771	0·206	−0·988	0·336	−1·185
8	−0·926	0·289	−0·863	0·164	−0·690	0·012	−0·524	−0·155	−0·432	−0·226	−0·339	−0·310	−0·265	−0·402	−0·176	−0·503	−0·015	−0·643	0·110	−0·810	0·247	−0·908
9	−0·717	0·235	−0·720	0·125	−0·595	−0·009	−0·476	−0·143	−0·399	−0·220	−0·330	−0·286	−0·259	−0·369	−0·170	−0·432	−0·048	−0·557	0·071	−0·679	0·193	−0·693
10	−0·589	0·196	−0·580	0·077	−0·500	−0·036	−0·399	−0·149	−0·348	−0·199	−0·295	−0·256	−0·241	−0·315	−0·173	−0·372	−0·074	−0·470	0·033	−0·548	0·131	−0·524
11	−0·389	0·110	−0·378	0·036	−0·336	−0·048	−0·254	−0·125	−0·268	−0·161	−0·236	−0·190	−0·174	−0·244	−0·136	−0·271	−0·074	−0·333	0·000	−0·357	0·086	−0·333
12	−0·322	0·074	−0·248	0·003	−0·239	−0·048	−0·206	−0·107	−0·177	−0·131	−0·165	−0·161	−0·145	−0·170	−0·127	−0·190	−0·071	−0·226	−0·029	−0·220	0·038	−0·250
13	−0·307	0·045	−0·139	−0·003	−0·130	−0·045	−0·127	−0·074	−0·103	−0·077	−0·091	−0·098	−0·083	−0·107	−0·071	−0·116	−0·053	−0·131	−0·018	−0·128	0·012	−0·244
14	−0·322	0·021	−0·103	−0·006	−0·068	−0·012	−0·047	−0·033	−0·041	−0·048	−0·044	−0·039	−0·035	−0·057	−0·041	−0·054	−0·024	−0·068	−0·015	−0·068	0·000	−0·235
15	−0·319	0·012	−0·035	−0·018	−0·009	0·012	0·006	0·018	−0·003	0·015	0·009	0·015	0·009	0·006	0·009	0·015	0·000	−0·006	0·006	−0·030	−0·018	−0·232
16	−0·304	−0·018	−0·029	0·018	0·018	0·029	0·041	0·047	0·044	0·050	0·035	0·056	0·035	0·050	0·024	0·050	0·018	0·041	0·006	−0·018	−0·041	−0·254

L = Lower Surface. U = Upper Surface.

TABLE 22

Wing and Body. Observed Pressure Coefficients at Station F

Tunnel Inci-dence	−16		−12		−8		−4		−2		0		2		4		8		12		16	
Point	L	U	L	U	L	U	L	U	L	U	L	U	L	U	L	U	L	U	L	U	L	U
1	−3·195	0·098	−2·112	0·062	−1·227	·0464	−0·496	0·336	−0·212	0·214	0·018	0·039	0·209	−0·196	0·348	−0·470	0·442	−1·155	0·330	−1·973	0·035	−2·807
2	−2·885	0·336	−2·006	0·452	−1·286	0·420	−0·640	0·256	−0·372	0·116	−0·136	−0·060	0·068	−0·271	0·227	−0·530	0·419	−1·125	0·451	−1·845	0·330	−2·777
3	−2·723	0·455	−1·920	0·461	−1·265	0·372	−0·687	0·152	−0·442	0·000	−0·230	−0·173	−0·038	−0·378	0·112	−0·622	0·345	−1·131	0·431	−1·744	0·428	−2·622
4	−2·507	0·458	−1·850	0·411	−1·260	0·283	−0·740	0·065	−0·513	−0·083	−0·316	−0·250	−0·147	−0·446	0·009	−0·658	0·254	−1·125	0·398	−1·685	0·442	−2·333
5	−1·826	0·420	−1·578	0·333	−1·147	0·179	−0·720	−0·051	−0·519	−0·173	−0·366	−0·318	−0·215	−0·473	−0·077	−0·646	0·142	−1·042	0·295	−1·455	0·398	−1·750
6	−1·445	0·354	−1·271	0·241	−1·003	0·101	−0·655	−0·104	−0·507	−0·211	−0·360	−0·324	−0·233	−0·449	−0·118	−0·595	0·071	−0·967	0·212	−1·205	0·339	−1·381
7	−1·024	0·229	−0·932	0·134	−0·746	−0·009	−0·566	−0·158	−0·454	−0·244	−0·369	−0·324	−0·263	−0·423	−0·180	−0·521	−0·024	−0·711	0·115	−0·857	0·233	−0·988
8	−0·753	0·164	−0·741	0·057	−0·619	−0·057	−0·470	−0·176	−0·408	−0·244	−0·330	−0·304	−0·256	−0·375	−0·202	−0·458	−0·071	−0·571	0·033	−0·693	0·131	−0·735
9	−0·560	0·098	−0·595	0·006	−0·503	−0·077	−0·408	−0·167	−0·366	−0·220	−0·295	−0·274	−0·238	−0·336	−0·202	−0·390	−0·104	−0·473	0·000	−0·571	0·089	−0·548
10	−0·440	0·057	−0·473	−0·018	−0·414	−0·098	−0·339	−0·170	−0·301	−0·205	−0·262	−0·241	−0·220	−0·298	−0·187	−0·336	−0·113	−0·402	−0·045	−0·455	0·036	−0·399
11	−0·263	0·015	−0·301	−0·042	−0·277	−0·089	−0·215	−0·134	−0·218	−0·152	−0·201	−0·170	−0·171	−0·199	−0·147	−0·211	−0·103	−0·259	−0·074	−0·286	−0·009	−0·250
12	−0·230	−0·021	−0·189	−0·048	−0·192	−0·086	−0·156	−0·101	−0·127	−0·113	−0·130	−0·122	−0·130	−0·131	−0·121	−0·146	−0·094	−0·167	−0·071	−0·164	−0·038	−0·187
13	−0·206	−0·039	−0·112	−0·062	−0·109	−0·068	−0·091	−0·077	−0·071	−0·065	−0·071	−0·062	−0·062	−0·077	−0·080	−0·071	−0·068	−0·095	−0·077	−0·095	−0·041	−0·187
14	−0·212	−0·030	−0·080	−0·051	−0·062	−0·048	−0·027	−0·024	−0·032	−0·012	−0·024	−0·012	−0·029	−0·012	−0·027	−0·015	−0·038	−0·045	−0·053	−0·051	−0·041	−0·196
15	−0·251	−0·051	−0·068	−0·042	−0·015	−0·015	0·009	0·009	0·018	0·018	0·018	0·024	0·021	0·021	0·018	0·024	−0·012	−0·009	−0·038	−0·054	−0·071	−0·250
16	−0·395	−0·080	−0·053	−0·024	−0·003	0·015	0·047	0·038	0·065	0·047	0·050	0·062	0·047	0·053	0·041	0·062	0·018	0·015	−0·024	−0·077	−0·077	−0·336

L = Lower surface. U = Upper surface.

TABLE 23

Wing and Body. Integrated Local Lift and Drag Coefficients, and Local Aerodynamic Centre

Station A. Chord 40 in.

Tunnel Incidence	Based on 40″ chord				Based on 12″ chord		Local a.c.
	Normal force	Tangential force	C_L	C_D	C_L	C_D	
− 16	− 0·303	0·0186	− 0·285	0·104	− 0·951	0·346	0·290
− 12	− 0·227	0·0230	− 0·216	0·072	− 0·721	0·238	0·284
− 8	− 0·156	0·0253	− 0·150	0·048	− 0·501	0·160	0·290
− 4	− 0·081	0·0262	− 0·079	0·032	− 0·262	0·108	0·315
− 2	− 0·044	0·0262	− 0·043	0·028	− 0·142	0·094	0·349
0	− 0·007	0·0246	− 0·007	0·025	− 0·022	0·082	—
2	0·029	0·0263	0·028	0·027	0·093	0·090	0·122
4	0·065	0·0262	0·064	0·030	0·212	0·100	0·231
8	0·135	0·0245	0·131	0·042	0·436	0·140	0·241
12	0·206	0·0228	0·197	0·063	0·658	0·211	0·257
16	0·289	0·0195	0·273	0·096	0·911	0·320	0·274

Station B. Chord 20·8 in.

Tunnel Incidence	Based on 20·8″ chord				Based on 12″ chord		Local a.c.
	Normal force	Tangential force	C_L	C_D	C_L	C_D	
− 16	− 0·477	− 0·0372	− 0·468	0·0997	− 0·810	0·1728	0·569
− 12	− 0·361	− 0·0192	− 0·357	0·0594	− 0·618	0·1030	0·570
− 8	− 0·236	− 0·0066	− 0·235	0·0284	− 0·407	0·0492	0·572
− 4	− 0·122	0·0013	− 0·121	0·0108	− 0·210	0·0187	0·577
− 2	− 0·069	0·0028	− 0·069	0·0058	− 0·119	0·0101	0·595
0	− 0·015	0·0029	− 0·015	0·0030	− 0·026	0·0052	—
2	0·044	0·0030	0·044	0·0042	0·077	0·0073	0·492
4	0·101	0·0017	0·100	0·0078	0·174	0·0135	0·530
8	0·215	− 0·0054	0·214	0·0227	0·370	0·0393	0·546
12	0·330	− 0·0212	0·327	0·0449	0·567	0·0778	0·554
16	0·453	− 0·0389	0·446	0·0835	0·774	0·1447	0·558

TABLE 24

Wing and Body. Integrated Local Lift and Drag Coefficients, and Local Aerodynamic Centre

Station C. Chord 12 in.

Tunnel incidence	Normal force	Tangential force	C_L	C_D	Local a.c.
− 16	− 1·001	− 0·1478	− 1·002	0·1427	0·295
− 12	− 0·747	− 0·0692	− 0·744	0·0941	0·278
− 8	− 0·503	− 0·0314	− 0·502	0·0432	0·273
− 4	− 0·254	− 0·0028	− 0·253	0·0171	0·265
− 2	− 0·142	0·0063	− 0·142	0·0125	0·289
0	− 0·025	0·0111	− 0·025	0·0113	—
2	0·099	0·0071	0·098	0·0097	0·217
4	0·219	− 0·0029	0·219	0·0105	0·241
8	0·454	− 0·0273	0·454	0·0322	0·259
12	0·693	− 0·0681	0·692	0·0714	0·266
16	0·956	− 0·1210	0·954	0·1388	0·287

Station D. Chord 12 in.

Tunnel incidence	Normal force	Tangential force	C_L	C_D	Local a.c.
− 16	− 0·900	− 0·1493	− 0·905	0·1124	0·279
− 12	− 0·663	− 0·0902	− 0·667	0·0554	0·245
− 8	− 0·460	− 0·0478	− 0·462	0·0208	0·236
− 4	− 0·244	− 0·0126	− 0·244	0·0066	0·238
− 2	− 0·135	− 0·0041	− 0·135	0·0018	0·230
0	− 0·034	0·0014	− 0·034	0·0017	—
2	0·080	− 0·0034	0·080	− 0·0013	0·162
4	0·178	− 0·0131	0·179	− 0·0022	0·166
8	0·404	− 0·0420	0·406	0·0111	0·221
12	0·609	− 0·0872	0·614	0·0360	0·224
16	0·858	− 0·1412	0·864	0·0931	0·270

TABLE 25

Wing and Body. Integrated Local Lift and Drag Coefficients, and Local Aerodynamic Centre

Station E. Chord 12 in.

Tunnel incidence	Normal force	Tangential force	C_L	C_D	Local a.c.
− 16	− 0·792	− 0·1528	− 0·802	0·0783	0·267
− 12	− 0·557	− 0·1060	− 0·566	0·0170	0·196
− 8	− 0·388	− 0·0507	− 0·392	0·0073	0·190
− 4	− 0·208	− 0·0164	− 0·208	0·0000	0·186
− 2	− 0·117	− 0·0045	− 0·117	0·0006	0·198
0	− 0·028	0·0002	− 0·028	0·0004	—
2	0·073	− 0·0005	0·073	0·0014	0·188
4	0·165	− 0·0105	0·166	− 0·0004	0·170
8	0·342	− 0·0412	0·344	0·0037	0·179
12	0·519	− 0·0844	0·526	0·0208	0·184
16	0·713	− 0·1350	0·723	0·0603	0·237

Station F. Chord 12 in.

Tunnel incidence	Normal force	Tangential force	C_L	C_D	Local a.c.
− 16	− 0·618	− 0·1217	− 0·628	0·0590	0·237
− 12	− 0·447	− 0·0919	− 0·456	0·0069	0·168
− 8	− 0·314	− 0·0475	− 0·317	− 0·0006	0·163
− 4	− 0·158	− 0·0173	− 0·159	− 0·0048	0·148
− 2	− 0·087	− 0·0087	− 0·087	− 0·0049	0·150
0	− 0·020	− 0·0048	− 0·020	− 0·0046	—
2	0·062	− 0·0076	0·062	− 0·0060	0·132
4	0·128	− 0·0153	0·128	− 0·0075	0·114
8	0·278	− 0·0395	0·281	− 0·0029	0·151
12	0·406	− 0·0700	0·411	0·0123	0·158
16	0·570	− 0·1062	0·577	0·0499	0·227

TABLE 26

Wing Only. Pressure Coefficients at Stations A, B, and D Adjusted for Zero Errors

	STATION A						STATION B			MEAN OF A AND B			STATION D		
	Mean for −2°	Mean for 0°	Mean for 2°	0° Lower and Upper	8°		0° Lower and Upper	8°		0° Lower and Upper	8°		0° Lower and Upper	8°	
Point					Upper	Lower		Upper	Lower		Upper	Lower		Upper	Lower
1	0·272	0·282	0·278	0·282	−0·296	0·632	0·314	−0·247	0·656	0·298	−0·272	0·644	0·090	−1·164	0·490
2	0·140	0·150	0·150	0·150	−0·408	0·552	0·178	−0·373	0·564	0·164	−0·390	0·558	−0·064	−1·168	0·467
3	0·042	0·050	0·048	0·050	−0·484	0·454	0·056	−0·482	0·478	0·053	−0·483	0·466	−0·182	−1·192	0·399
4	−0·040	−0·036	−0·035	−0·036	−0·542	0·380	−0·027	−0·533	0·386	−0·032	−0·538	0·383	−0·262	−1·168	0·326
5	−0·120	−0·120	−0·122	−0·120	−0·582	0·313	−0·111	−0·564	0·292	−0·116	−0·573	0·302	−0·316	−1·090	0·226
6	−0·146	−0·144	−0·142	−0·144	−0·566	0·234	−0·156	−0·575	0·228	−0·150	−0·570	0·231	−0·330	−1·048	0·166
7	−0·196	−0·196	−0·191	−0·196	−0·563	0·151	−0·199	−0·575	0·150	−0·198	−0·569	0·150	−0·357	−0·802	0·072
8	−0·226	−0·223	−0·224	−0·223	−0·548	0·098	−0·218	−0·542	0·100	−0·220	−0·545	0·099	−0·340	−0·700	0·010
9	−0·238	−0·236	−0·242	−0·236	−0·524	0·058	−0·238	−0·530	0·060	−0·237	−0·527	0·059	−0·316	−0·598	−0·016
10	−0·242	−0·242	−0·241	−0·242	−0·502	0·040	−0·242	−0·502	0·040	−0·242	−0·502	0·040	−0·290	−0·526	−0·032
11	−0·238	−0·238	−0·241	−0·238	−0·444	0·012	−0·238	−0·448	0·009	−0·238	−0·446	0·010	−0·229	−0·375	−0·034
12	−0·217	−0·216	−0·216	−0·216	−0·394	−0·006	−0·217	−0·392	−0·004	−0·216	−0·393	−0·005	−0·174	−0·260	−0·020
13	−0·182	−0·180	−0·181	−0·180	−0·325	0·000	−0·174	−0·325	0·000	−0·177	−0·325	0·000	−0·092	−0·175	−0·015
14	−0·131	−0·138	−0·134	−0·138	−0·253	0·009	−0·138	−0·253	0·010	−0·138	−0·253	0·010	−0·050	−0·096	0·003
15	−0·080	−0·084	−0·081	−0·084	−0·174	0·032	−0·082	−0·175	0·032	−0·083	−0·174	0·032	−0·010	−0·042	0·024
16	−0·030	−0·026	−0·027	−0·026	−0·081	0·050	−0·015	−0·070	0·052	−0·020	−0·076	0·051	0·034	0·014	0·044

TABLE 27

Wing and Body. Pressure Coefficients at Stations A and D Adjusted for Zero Errors

Point	STATION A			STATION D		
	0° Upper and lower	8°		0° Upper and lower	8°	
		Upper	Lower		Upper	Lower
0	0·988	0·950	0·950			
1	0·301	0·000	0·568	0·070	− 1·276	0·456
2	0·134	− 0·124	0·390	− 0·082	− 1·274	0·466
3	0·038	− 0·174	0·264	− 0·180	− 1·282	0·406
4	0·008	− 0·174	0·206	− 0·286	− 1·292	0·336
5	− 0·040	− 0·187	0·136	− 0·329	− 1·168	0·224
6	− 0·074	− 0·197	0·068	− 0·361	− 1·112	0·150
7	− 0·088	− 0·180	0·046	− 0·372	− 0·862	0·062
8	− 0·113	− 0·180	0·006	− 0·368	− 0·740	− 0·002
9	− 0·118	− 0·186	− 0·010	− 0·352	− 0·650	− 0·038
10	− 0·106	− 0·190	− 0·012	− 0·319	− 0·575	− 0·049
11	− 0·136	− 0·242	− 0·004	− 0·254	− 0·423	− 0·052
12	− 0·156	− 0·254	− 0·028	− 0·206	− 0·302	− 0·055
13	− 0·092	− 0·151	− 0·034			− 0·028
14	− 0·043	− 0·040	− 0·009	− 0·052	− 0·122	0·000
15	0·020	0·030	0·015	− 0·010	− 0·052	0·024
16	0·071	0·080	0·062	0·026	0·004	0·030
17	0·088	0·100	0·084			

(22974)

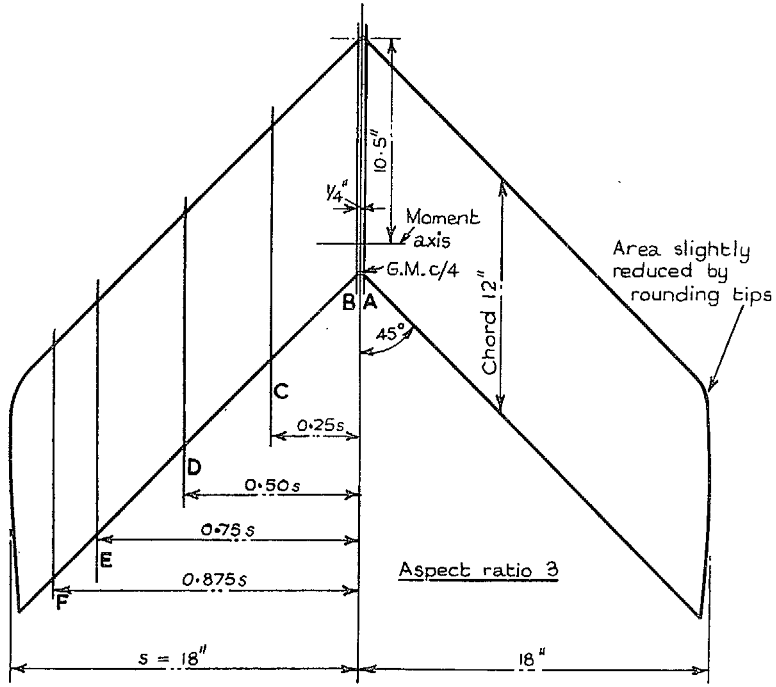

FIG. 1. Symmetrical swept-back wing. Pressure plotting stations.

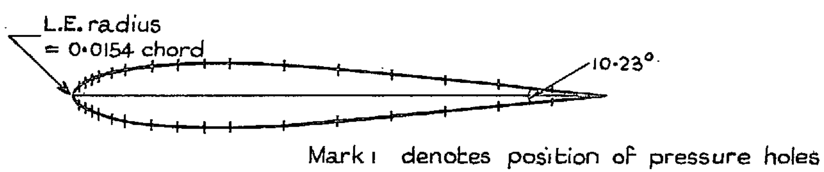

FIG. 2. Piercy symmetrical section.

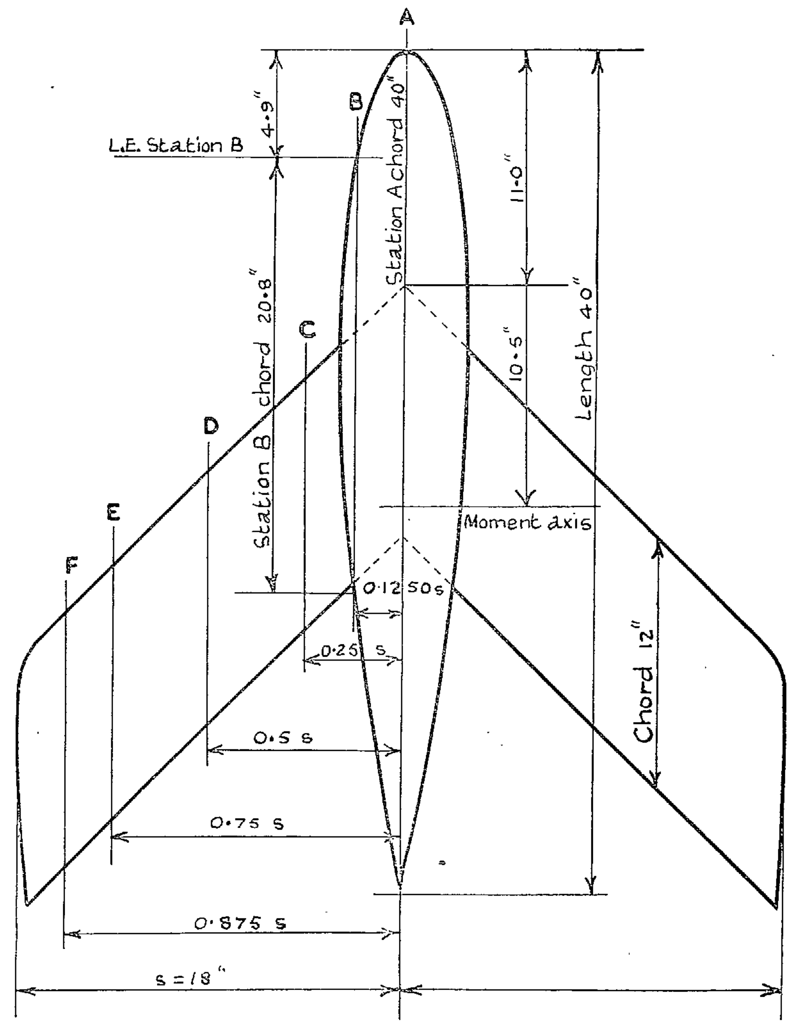

FIG. 3. Symmetrical swept-back wing and body: pressure plotting stations.

(22974)

3F

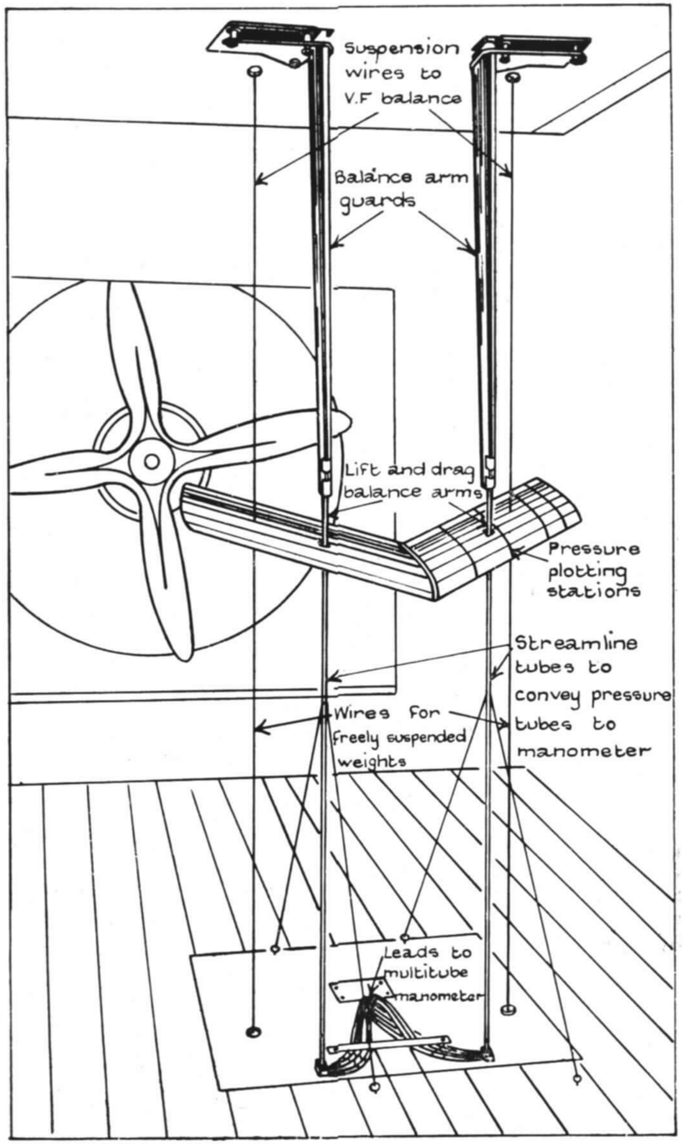

FIG. 4. Arrangement of pressure plotting wing in 7 ft No. 2 Wind Tunnel.

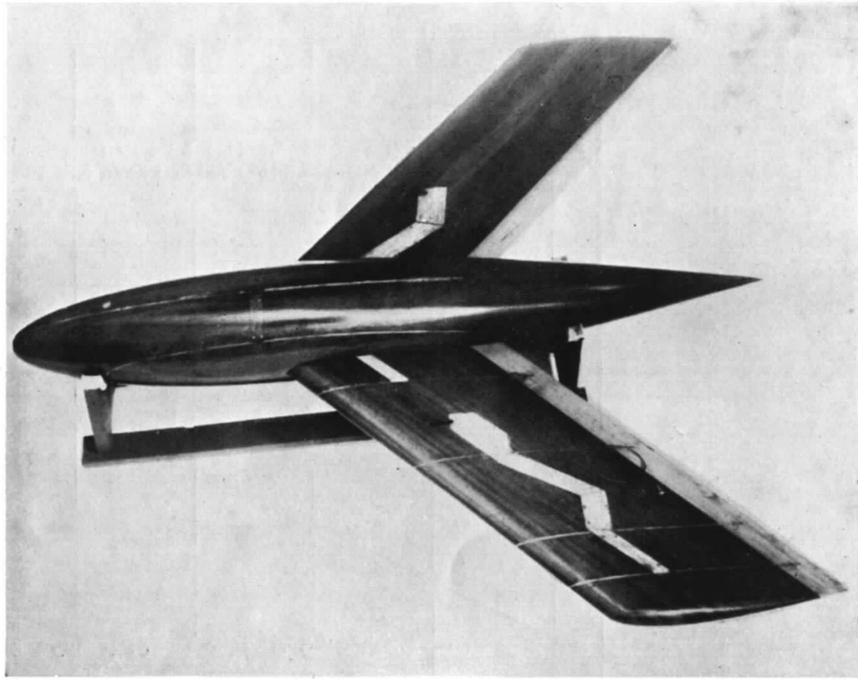

FIG. 5.

C*

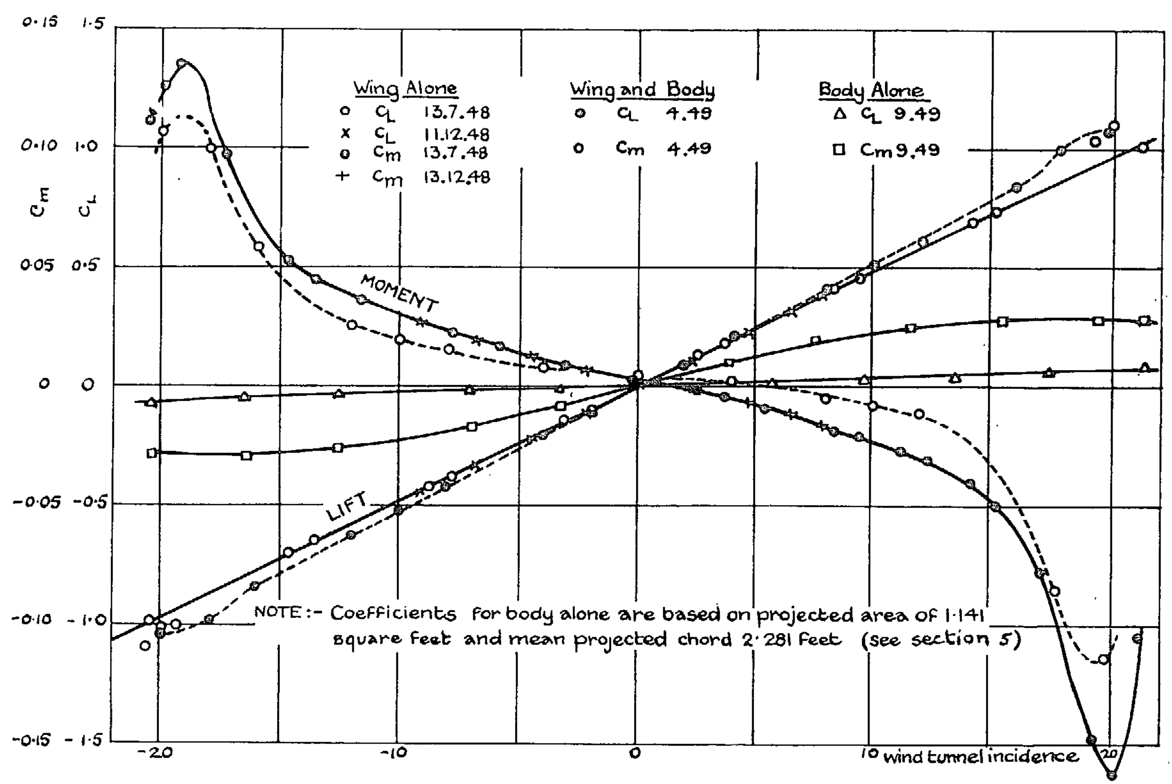

FIG. 6. Swept-back wing: balance measurements of lift and moment.

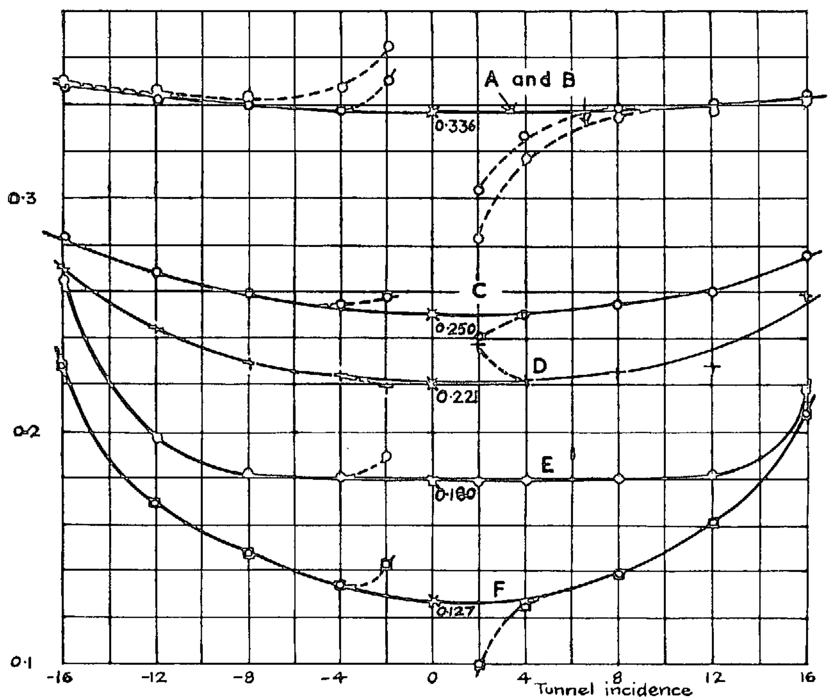

FIG. 7. Wing alone. Local centre of pressure of normal force plotted against incidence for stations A to F.

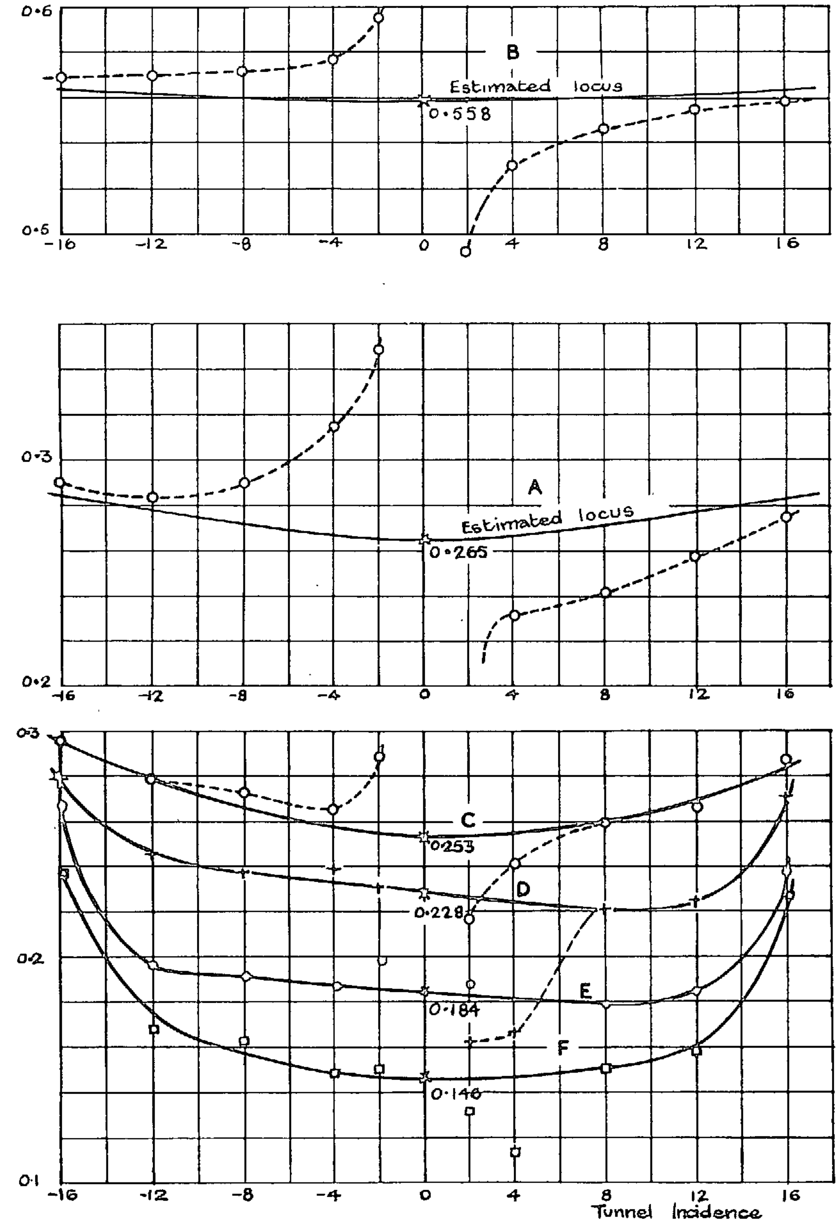

FIG. 8. Wing and body. Local centre of pressure of normal force plotted against incidence for stations A to F.

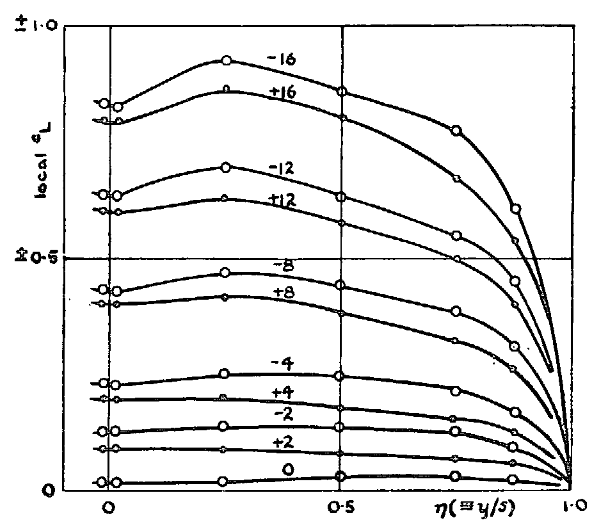

Wing only. Local lift coefficient plotted against spanwise position for various incidences.

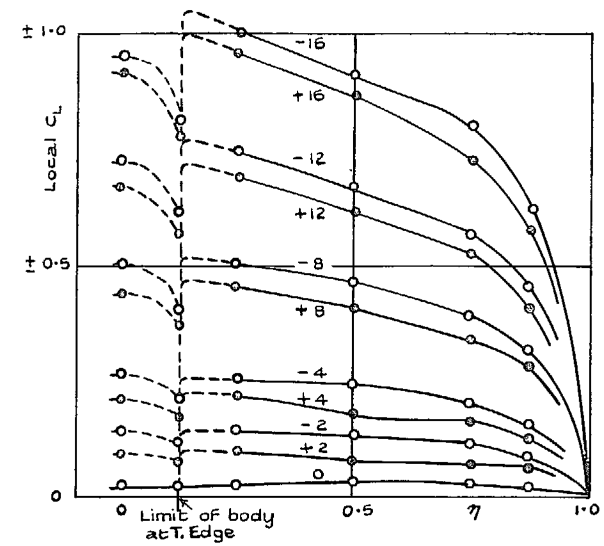

Wing and body. Local lift coefficient based on 12 in. chord plotted against spanwise position for various incidences.

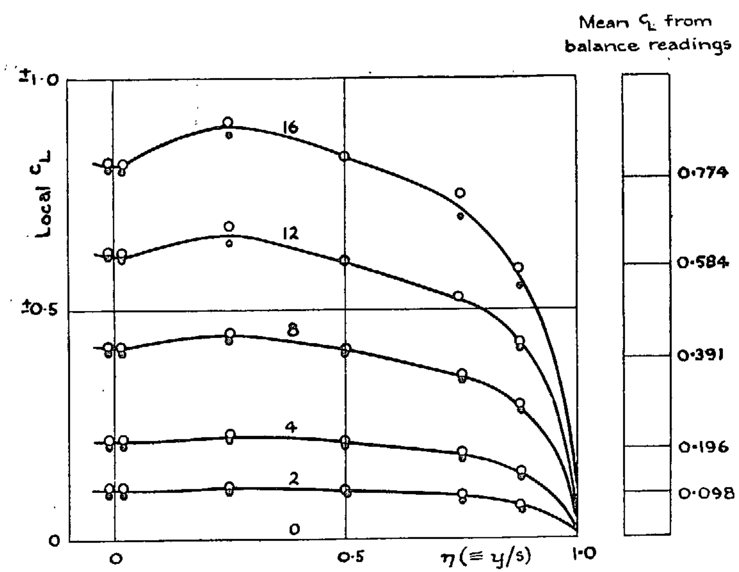

Wing only. Relative local lift coefficients plotted against spanwise position. Chord 12 in.

FIG. 9.

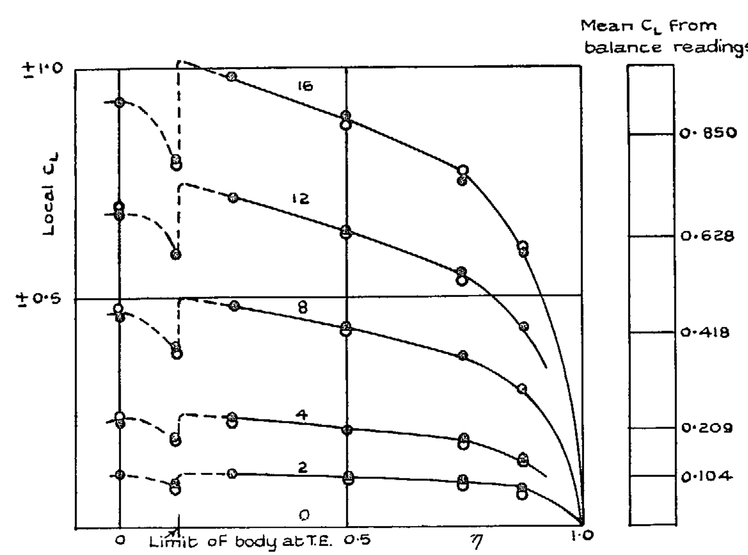

Wing and body. Relative local lift coefficients based on 12 in. chord plotted against spanwise position.

FIG. 10.

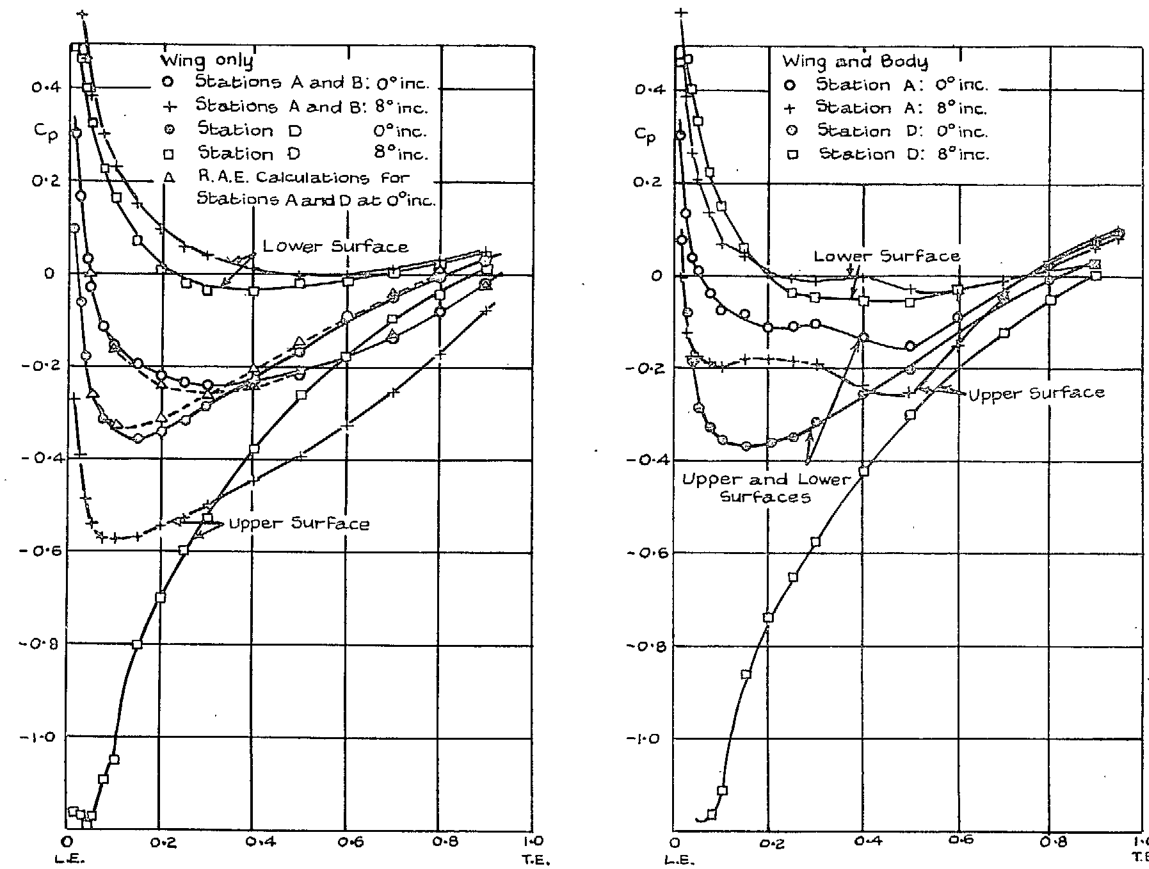

FIG. 11. Observed chordwise pressure distribution at two stations on wing alone and wing with body.

(22974) Wt. 15-680 K9 10/53 F. M. & S.

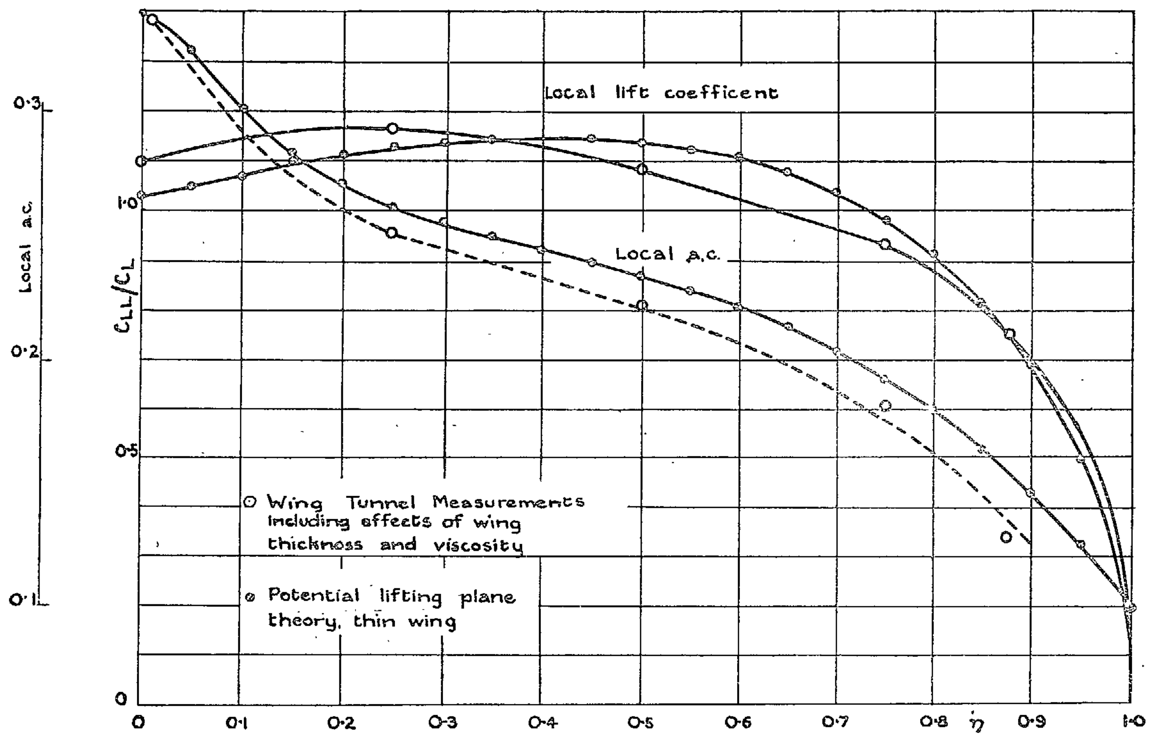

FIG. 12. Aerodynamic loading of a swept-back wing.

PRINTED IN GREAT BRITAIN

R. & M. No. 2741
(12,647)
A.R.C. Technical Report

Publications of the Aeronautical Research Council

S.O. Code No. 23-2741